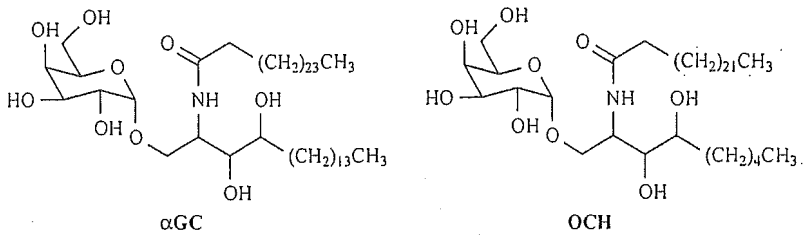

Fig. (1). Structure of α-galactosylceramide (α-GC) and OCH. The α-anomeric conformation of sugar moiety, the configuration of the 2-hydroxyl group on the sugar moiety, 3,4 –hydroxyl groups of the phytosphingoshine are important for NKT cell recognition of α-GC [10]. The OCH analogs has a shorter shpingosine chain.

NKT cells are comprised of two subsets; $CD4^+$ or $CD4^-$ $CD8^-$ (double negative DN). Although the tissue distribution of NKT cells varies, they are most frequent in the liver and bone marrow, and less abundant in the spleen. Whereas human and mouse NKT cells share many characteristics, the frequency is much lower in humans [2]. Moreover, $CD4^+$ and DN NKT cells appear different in terms of cytokine production in humans but not in mice [5,6]. The $CD4^+$ subset of human NKT cells produces both Th1 and Th2 cytokines upon antigen stimulation, whereas the DN subset produces Th1 cytokines and upregulates production of perforin after exposure to cytokines [6].

NKT cells are selected by, and restricted to CD1d. This unique class of antigen-presenting molecules has been highly conserved through mammalian evolution. It is speculated that self glycolipid antigens probably function as activating ligands for NKT cells due to the self-reactivity of NKT cells and the activated memory phenotype of NKT cells isolated from human umbilical-cord blood [7,8] and germ-fee mice [9].

α-GC is a synthetic glycolipid originally isolated from marine sponges *Agelas mauritanius*, and later, a synthetic analog of this compound was developed for experimental studies and clinical trials (Fig. (1)) [10]. α-GC has been shown to be a potent stimulator of both murine and human NKT cells [10-12]. NKT cells respond to sphingolipids substituted with an α-linked galactose or glucose, but not α-linked mannose and sphingolipids containing β-linked galactose or glucose [10]. Sphingolipids containing β-linked sugars resemble common mammalian lipids, whereas α-glycosyl sphingolipids have not been found in normal mammalian tissues. Recently, GD3, a ganglioside expressed on human tumors of neuroectodermal origin has been reported to be recognized by NKT cells [13]. Similar to α-GC, GD3 is not expressed or expressed at low levels on normal tissues.

REGULATION OF CYTOKINE PRODUCTION BY NKT CELLS

NKT cells are characterized by exhibiting a pre-activated phenotype in physiological conditions, being $CD69^+$, $CD62L^{low}$, and $CD44^{high}$. Consistent with the pre-activation status, NKT cells release large amounts of cytokines including IL-4 and IFN-γ promptly upon antigen stimulation and affect the functions of neighboring cell populations such as T cells, B cells, NK cells and dendritic cells (Fig. (2)). [2,5,6]. The mechanisms underlying their rapid cytokine production or their distinct cytokine patterns remain unknown. Recently, Stetson DB *et al.* reported that NKT cells contained 1,000-fold more IL-4 message and 200-fold more IFN-γ message than naive $CD4^+$T cells and levels of H3 acetylation at both the IL-4 and IFN-γ promoters [14]. These chromatin modifications at cytokine genes that correlated with the presence of abundant cytokine mRNAs are similar to differentiated helper T cells such as Th1 or Th2 cells. During differentiation, one set of genes is epigenetically activated and the other is silenced in Th1 or Th2 cells. It is thought that lineage-specific transcription factors such as GATA-3 and T-bet function to maintain and increase the accessibility of one cytokine locus while suppressing or silencing the other in the differentiated cells [15]. Interestingly, NKT cells express both GATA-3 and T-bet allowing hyperacetylation at the IL-4 and IFN-γ promoters (Oki S and Miyake S, unpublished observations).

α-GC induces a variety of cytokines including IFN-γ, IL-2, tumor necrotic factor-α, IL-4 and IL-13 from NKT cells. In contrast, a sphingosine-truncated analogs of α-GC, such as OCH, stimulates NKT cells to preferentially produce IL-4, IL-13. It is important to understand the mechanisms how OCH can stimulate NKT cells to produce Th2 cytokines selectively. IFN-γ production by NKT cells seems to correlate with the stability of glycolipid ligands to bind to the CD1d molecule, and the binding stability correlates with the length of sphingosine chains. Thus OCH binds to CD1d molecule less stably compared to α-GC because of the truncation of sphingosine chain and is therefore not able to sustain TCR stimulation, resulting in preferential production of IL-4 from NKT cells [16]. Given that IL-4 secretion consistently precedes IFN-γ production by NKT cells after TCR ligation, we speculated a critical difference in the upstream transcriptional requirements for the IFN-γ and the IL-4 genes in NKT cells. In support of this speculation, cyclohexamide treatment inhibited the transcription of IFN-γ, but not that of IL-4. In contrast, transcription of both cytokines was abolished by cyclosporine A treatment, indicating that TCR-mediated activation of nuclear factor of activated T cells (NF-AT) is essential for the production of both cytokines. Interestingly, IFN-γ production by NKT cells requires longer TCR stimulation than required for IL-4 when stimulated with immobilized anti-CD3 antibody. TCR stimulation-dependent NF-AT activation is regulated in a manner quite sensitive to change of Ca^{2+} concentration [17]. Thus activated NF-AT might be no longer available for effective IFN-γ transcription due to its quick export from the nucleus after the short duration of TCR stimulation by OCH.

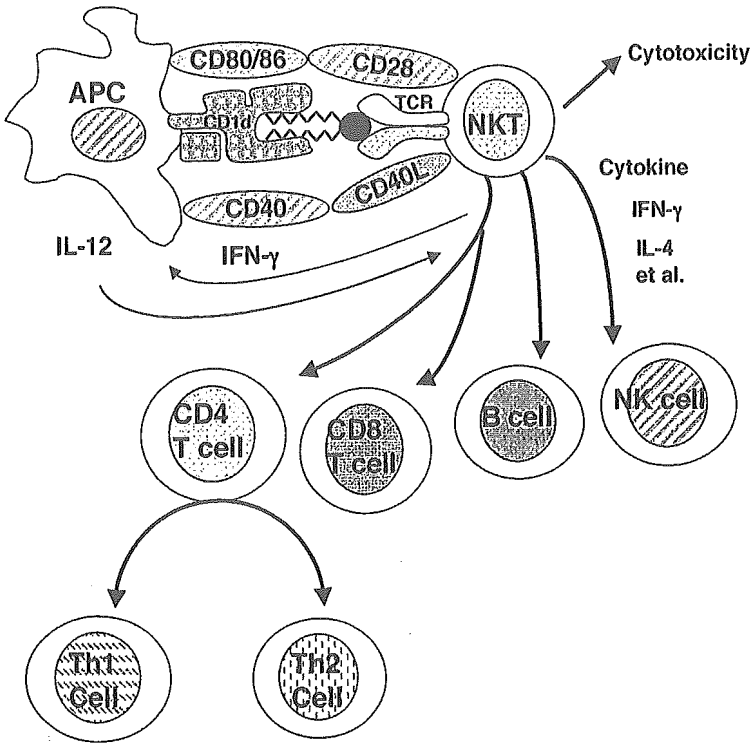

Fig. (2). A model of NKT cell activation and their interactions with other subsets of cells. NKT cells recognize glycolipid ligand presented by CD1d molecule. After stimulation, NKT cells produce a variety of cytokines and exert effector functions. NKT cells might be important for the differentiation of $CD4^+$ T cells into Th1 or Th2 cells, maturation of dendritic cells and activation of B cells and natural killer cells.

Given that *in vivo* administration of soluble OCH and α–GC induces cytokine production by NKT cells within 90 m, stimulation of NKT cells after *in vivo* injection of α–GC or OCH probably occurs without intracellular processing. In fact, when it is presented by antigen presenting cells (APCs) expressing a cytoplasmic tail mutant of the CD1d molecule which is unable to undergo endosomal/lysosomal sorting, the stability of glycolipid antigen binding to CD1d correlated with its length of sphingosine chain. However, when we used APCs expressing wild type CD1d and pulsed antigens for longer time period, the uptake of glycolipids and subsequent endosomal/lysosomal assembly with CD1d, strengthened the interaction of glycolipids with CD1d and abolished the correlation of the binding stability to CD1d and lipid tail length. When we used bone marrow-derived mature dendritic cells as APCs, there was no significant difference between long-term pulsed OCH and α–GC in the ability to induce IFN-γ by freshly isolated NKT cells *in vitro* (Oki S. and Miyake S., unpublished observation).

GLYCOLIPID THERAPIES FOR AUTOIMMUNE DISEASE MODELS

Experimental Autoimmune Encephalomyelitis

EAE is an autoimmune inflammatory disease affecting the central nervous system (CNS) that serves as a model for MS. EAE can be induced in susceptible mouse strains by immunization with CNS proteins or peptides in adjuvant or by the passive transfer of T cells reactive against such CNS antigens. Studies with animal models has suggested that myelin-specific Th1 cells secreting IFN-γ, tumor necrotic factor-α and IL-2 mediate EAE, whereas myelin-specific Th2 cells producing IL-4 and Il-10 play a protective role [18]. Therefore administration of Th2 cytokines to control the disease was considered for clinical use. However, clinical trails of recombinant cytokines, except for IFN-β, have mostly failed because of accompanying side effects. Recently, local delivery of Th2 cytokines, using autoimmune T cells, using hybridomas or fibroblasts transfected with genes encoding anti-inflammatory cytokines was found to be effective in the suppression of EAE [19,20]. However, this strategy seems to be difficult for clinical treatment without major technical advances in introducing particular genes into these cells and in culturing autoimmune T cells. Since NKT cells are known to rapidly invade and accumulate in inflammatory lesions in a manner similar to inflammatory cells and produce cytokines, the stimulation of NKT cells to produce Th2 cytokines would be a powerful strategy to deliver protective cytokines to autoimmune-mediated inflammatory lesions. Nevertheless we observed only a marginal effect of α-GC on the clinical course of EAE induced in C57BL/6 (B6) mice with myelin oligodendrocyte glycoprotein (MOG) derived peptides even though we tried protocols with varying doses of α-GC or different timing of injection [21,22]. Since NKT cells produce both IFN-γ and IL-4 upon stimulation with α-GC, we postulated that α-GC could not prevent EAE because NKT cell-derived IFN-γ would mask the protective effect of the IL-4 simultaneously produced by NKT

cells. We showed several lines of evidence supporting this idea [21]. First, α-GC treatment inhibited EAE induced in IFN-γ knockout mice. Secondly, α-GC treatment augmented the clinical sings of EAE induced in IL-4 knockout mice. Thirdly, blockade of CD86 polarized NKT cells toward a Th2-like phenotype with concomitant suppression of EAE, and activation of APCs by treatment with stimulatory anti-CD40 mAb biased them towards a Th1-like phenotype and exacerbated EAE. As such, EAE could be prevented when ligand stimulation would lead to selective production of Th2 cytokines by NKT cells *in vivo*. Thus we synthesized several analogs of α-GC and found that a sphingosine-truncated analog, OCH, induced selective IL-4 production by NKT cells (Fig. (3)). As expected, administration of OCH prevented development of EAE in both clinical and pathological parameters. The inhibitory effect of OCH was not observed for EAE induced either in NKT cell deficient or IL-4 knockout mice, confirming that IL-4 produced by NKT cells is critical for OCH-mediated suppression on EAE [22].

By contrast, two more reports have shown that α-GC protects mice against EAE when delivered in the immunization protocol (MOG_{35-55} and complete Freund's adjuvant [CFA]) with subsequent multiple intraperitoneal injection or by using a single injection at the day of induction of EAE [23,24]. More recently, Furlan R *et al.* showed that EAE was suppressed only when α-GC was administered at the time of immunization subcutaneously mixed with CFA but not administered intraperitoneally [25]. Although it is not clear the difference among these studies, the role of NKT cells in the pathogenesis or prevention of autoimmunity in CNS may depend on the stage of disease and the associated cytokine milieu, the timing or the route of administration. These parameters are critical to modulate diseases.

In addition to B6 mice, SJL mice are highly susceptible to EAE and EAE induced by immunization with proteolipid protein derived peptides $PLP_{139-151}$ is used as a remitting-relapsing MS model. In the context of NKT cells, SJL mice have been reported to be markedly diminished in number and cytokine production upon activation [26]. Singh AK *et al.* reported that SJL mice responded poorly to treatment with α-GC [24]. When SJL mice were treated with α–GC, the morbidity and mortality were exacerbated although the onset of disease was delayed. By contrast, a multiple injection of OCH protected SJL mice against EAE (Miyake S and Yamamura T, unpublished observation). Furthermore, OCH protected SJL mice against the relapse of EAE, suggesting

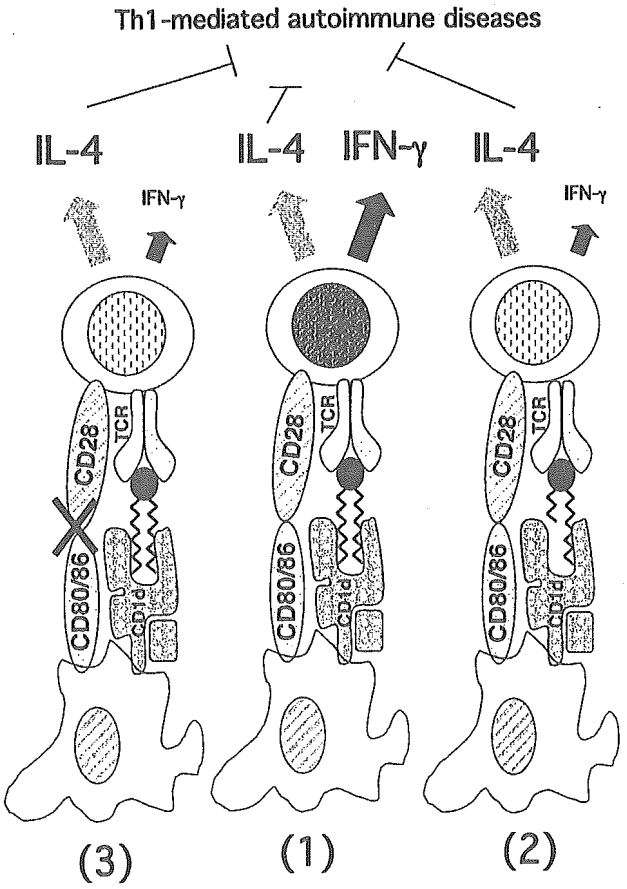

Fig. (3). Modulation of NKT cell cytokine production by an altered ligand or by co-stimulator blockade. 1) α-GC stimulates NKT cells to produce both anti-inflammatory (e.g. IL-4 and IL-10) and pro-inflammatory (e.g. IFN-γ) factors. This response can be modified by 2) stimulation with an altered ligand such as OCH or 3) stimulation in the absence of CD28/B7.2 co-stimulation. These modifications are potentially important therapeutic approach to suppress Th1-mediated autoimmune diseases.

that OCH holds possibilities as a therapeutic agent to prevent relapses for MS.

Glycolipid Therapy for Collagen-induced Arthritis

RA is an autoimmune disease characterized by persistent inflammation of joints resulting progressive destruction of cartilage and bone. Although its precise etiology is not clearly understood, cumulative evidence suggests that Th1 cells exacerbate disease, whereas Th2 cells suppress arthritis [27]. Given that NKT stimulation with OCH suppressed Th1-mediated diseases such as EAE, OCH might be an effective therapeutic reagent for CIA which serves as an animal model for RA. We have demonstrated that OCH administration inhibited the clinical course of CIA induced in B6 mice by immunization with the chicken type II collagen [28]. Histological analysis revealed that OCH treatment protected against infiltration of inflammatory cells and destruction of cartilage and bone. The suppressive effect of OCH was not observed for CIA induced either in CD1d knockout mice or in Jα18 knockout mice deficient in NKT cells. We also observed OCH suppressed CIA induced in DBA/1J mice immunized with bovine type II collagen. Moreover, injection of OCH strongly suppressed CIA in SJL mice even though these mice have defects in numbers and functions of NKT cells, and even after the arthritis had already developed. By contrast, administration of α-GC didn't suppress arthritis in any of these three models. Suppression of arthritis was associated with the elevation of IgG1:IgG2a ratio indicating the Th2 bias of type II collagen-reactive T cells. Injection of neutralizing antibody to either IL-10 or IL-4 reversed the beneficial effect of OCH treatment. These results imply that IL-10 and IL-4 are critical in the OCH-mediated suppression of CIA and are consistent with our idea that OCH modulated CIA by stimulating the production of Th2 cytokines from NKT cells although the source of IL-10 remains to be elucidated. Since OCH seems a potential therapeutical tool to suppress arthritis, the role of NKT cells in the natural course of arthritis should be clarified in the future.

Glycolipid Therapy for Autoimmune Diabetes in NOD Mice

Nonobese diabetic (NOD) mice develop a spontaneous autoimmune diabetes similar to the human T1D. Autoimmune destruction of β cells is preceded by infiltration of pancreatic islets by macrophages, B cells and T lymphocytes [29,30]. Many studies have indicated that Th1 type $CD4^+$ cells and $CD8^+$ T cells have been implicated in the development of diabetes in the NOD mouse. In parallel with these effector cells, the regulatory cells including NKT cells have been suggested to inhibit the development of diabetes. Although the mechanisms of suppressive effect of these regulatory T cells are not fully understood, it is believed that an imbalance between autoreactive effector T cells and regulatory T cells may trigger the development of destructive insulitis and diabetes [28].

Studies have indicated that NOD mice were deficient in the number and function of NKT cells [31]. Although the correlation between a defect in NKT cells and the susceptibility of diabetes in NOD mice is still debated [3,32,33], the putative involvement of NKT cells in the control of islet β-cell reactive T cells in NOD mice was suggested by prevention of diabetes following infusion of NKT cell enriched thymocytes preparations [34] and by the increase of NKT cells in Vα14Jα281 transgenic NOD mice [35].

Several recent papers investigated the effect of treating NOD mice with α-GC [33,35-38]. When started around three or four weeks of age, repeated injections at least once a week delayed the onset and reduced the incidence of diabetes. After treatment, splenocytes from NOD mice produced a greater amount of IL-4 in response to islet antigens and the IgG1/IgG2a (Th2/Th1) ratio of anti-GAD antibody increased. Thus it appears that the mechanism of protection is similar to that observed by increasing the numbers of NKT cells in NOD mice and by α–GC treatment in other autoimmune disease models such as EAE and CIA. This effect was auto-antigen specific as no difference was observed in the immune response to ovalbumin [36]. However, the mechanism in which glycolipid treatment induces an auto-antigen specific switch in the immune response of NOD mice is unclear. We also observed the protective effect of OCH treatment in NOD diabetic mice in addition to α-GC treatment. The protective effect for insulitis by OCH was more profound compared to that by α-GC [56].

GLYCOLIPID THERAPY FOR MOUSE MODELS OF SYSTEMIC LUPUS ERYTHEMATOSUS

It has been reported that a selective reduction in $NK1.1^+$ T cells precedes the development of autoimmunity in MLR lpr/lpr mice. Mieza MA *et al.* also found a decrease in the expression of invariant Vα14 TCR mRNA of NKT cells before the onset of lymphocyte accumulation and autoimmune disease in MRL lpr/lpr mice, C3H gld/gld and NB/W F1 mice when compared to control mice [39]. Recently, Zeng D *et al.* demonstrated that treatment of NZB/W F1 mice with anti-CD1d monoclonal antibody augmented Th2-type responses, increased serum levels of IgE, decreased levels of IgG2a and IgG2a anti-double-stranded DNA (dsDNA) antibodies, and ameliorated lupus [40]. They also showed that multiple injection of α-GC induced an enhanced Th1-type response and exacerbated lupus associated with decreased serum levels of IgE and increased levels of IgG2a and IgG2a anti-ds DNA antibodies. This exacerbation of disease was associated with reduced IL-4 and tumor necrotic factor-α production and expansion of marginal zone B cells. These results suggested that activation of NKT cells augmented Th1-type responses and autoantibody production that contribute to lupus development in NZB/W F1 mice. In contrast, Yang JQ *et al.* reported that pristine-induced lupus nephritis was accelerated when induced in CD1d deficient mice [41]. They also demonstrated that repeated injection of α-GC resulted in the expansion of NKT cells and ameliorated dermatitis in MRL lpr/lpr mice [42]. Thus they postulated that NKT cells may play a protective role in lupus models. Since lupus models are not simply explained by only Th1-mediated or Th2-mediated pathology, the complexity of these models may explain the differences in results in these studies.

NKT Cells in Human Autoimmune Diseases

Multiple Sclerosis

MS is an autoimmune demyelinating disease of the CNS. Illes Z *et al.* reported a reduction in Vα24Jα18 cells among $Vα24^+$ cells from the peripheral blood of patients with MS compared to healthy subjects using single-strand conformation polymorphism method to detect TCR gene rearrangements [43]. Van der Vliet *et al.* showed a decrease in the number of NKT cells by screening of $Vα24^+Vβ11^+$ cells in the blood [44]. Araki M *et al.* demonstrated that DN NKT cells in the periphery were greatly reduced in remission whereas the reduction of $CD4^+$ NKT cells was marginal [45]. Furthermore $CD4^+$ NKT line cells expanded from MS in remission produced a larger amount of IL-4 than those from healthy subjects or from MS in relapse. Therefore, we speculated that the Th2 bias of $CD4^+$ NKT cells may play a role in the regulation of Th1 type autoantigen reactive T cells. In contrast, Gausilng *et al.* did not find a significant difference in the number of DN $Vα24^+$ NKT cells in PBL between from MS patients and from healthy controls [46]. The basis for the discrepancy between the number of NKT cells among these studies is not clear. Considering that the proportion of Vα24Jα18 T cells in normal individuals varies among studies, it may not be easy to compare these studies.

Type I Diabetes

Studies of the frequency of human NKT cells in PBMCs in patients with T1D have had conflicting results. In initial studies, Wilson B *et al.* studied identical twin/triplet sets discordant for disease, and reported that diabetic siblings have lower frequencies of DN Vα24Jα18 T cells in their peripheral blood than non-diabetic siblings [47]. In addition, Kukreja AG *et al.* showed a reduction in the number of NKT cells in newly diagnosed patients [48]. However, more recent papers reported unaltered or increased NKT cells in recent-onset patients with type I diabetes [49,50]. Wilson B *et al.* also showed that DN Vα24Jα18 T cell clones isolated from diabetics had an impaired ability to produce IL-4 [47]. In contrast, Lee PT *et al.* reported IL-4 production by NKT cells was similar among these groups as assessed by intracytoplasmic staining following short-term PMA and ionomycin stimulation [49]. At this stage, it is hard to interpret the discrepancies between these results, since the methods for detecting NKT cells and the functional assays used differ between these studies.

Systemic Autoimmune Disease

Sumida and colleagues found that αβ+ DN T cells were increased in Scleroderma patients and that there was oligoclonal expansion of $Vα24^+TCR^+$ cell among these cells [51]. Although the invariant Vα24Jα18 T cells were dominant among these cells from healthy donors, invariant Vα24Jα18 T cells were replaced by clones with other Vα24 TCR^+ cells in Scleroderma patients. In addition, Maeda *et al.* have reported the expansion of non-invariant Vα24 TCR^+ cells but not Vα24Jα18 T cells in the synovium of RA patients [52]. Similar to this study, these authors observed the expansion of non-invariant Vα24 TCR^+ clones in patients with active SLE [53, 54]. Furthermore, following predonisolone therapy, Vα24Jα18 T cells increased among Vα24 TCR^+ cells. The recovery of Vα24Jα18 T cells in patients with predonisolone therapy was also observed among patients with MS (Araki M and Yamamura T, unpublished observation). Kojo S *et al.* and other groups investigated the number of NKT cells using Vα24 and Vβ11 mAb to detect NKT cells in patients with several different autoimmune diseases, including SLE, Scleroderma and RA [43, 55]. They found lower numbers of $Vα24^+Vβ11^+$ NKT cells in the peripheral blood than controls. Kojo S *et al.* also showed in this study that half of the patients with autoimmune disease responded to α-GC in culture.

PROSPECTS FOR GLYCOLIPID THERAPY FOR AUTOIMMUNE DISEASES

It remains unclear whether the defect in NKT cells is causal for autoimmune disease or occur as a secondary consequence of the autoimmune process. However, given the efficacy of OCH and α-GC in mouse models, stimulation of NKT cells with glycolipid antigens seems to be an attractive strategy for the treatment of autoimmune diseases. Although several studies have shown that administration of α-GC caused liver damage, the hepatotoxicity was minimal in Phase I trials of α-GC for patients with cancer. Given the lack of severe toxicity in humans, it seems reasonable to use glycolipids for the prevention or therapy of selected human autoimmune disorders. α-GC has been shown to exacerbate EAE, depending on the strain of mouse and stage of disease tested and to have only a marginal effect on CIA. In this situation, treatment with OCH might be preferable to α-GC for Th1-mediated diseases such as MS, type I diabetes and RA, as OCH elicits a predominantly IL-4 response rather than IFN-γ in contrast to α-GC, which might afford greater protection from EAE and MS.

Both rodent and human NKT ells have been reported to recognize α-GC in the context of CD1d. OCH also stimulates human NKT cells, particularly $CD4^+$ NKT cells, and OCH stimulation induces more Th2 cytokine production from NKT cells compared to α-GC stimulation (Araki M and Yamamura T, unpublished observation). The evolutionary conservation and the homogeneous ligand specificity of NKT cells allow us to apply a glycolipid ligand like OCH for the treatment of human disease without considering species barrier or genetic heterogeneity of humans.

CONCLUSION

In this review, we have discussed the supporting data for the role of NKT cells in the regulation of autoimmune diseases. Ligand stimulation of NKT cells is an attractive strategy for prevention or treatment of autoimmune diseases. However, the mechanisms by which NKT cells exert their immunoregulatory functions are still largely unknown and a number of questions require further investigation including the mechanism to recruit NKT cells and control its functions at inflammatory sites and the interaction of other subsets of cells. To clarify the nature of natural ligands for NKT cells is one of the major questions and it could be an interesting natural source of useful ligands for CD1-restricted regulatory cells.

ABBREVIATIONS

NKT = Natural killer T

MHC = Major histocompatibility complex

α-GC = α-galactosylceramide

EAE = Experimental autoimmune encephalomyelitis

CIA = Collagen induced arthritis

Th = T helper

IL = Interleukin

IFN = Interferon

T1D = Type 1 diabetes

MS = Multiple sclerosis

RA = Rheumatoid arthritis

TCR = T cell receptor

DN = Double negative

NF-AT = Nuclear factor of activated T cells

APC = Antigen presenting cell

CNS = Central nervous system

B6 = C57BL/6

MOG = Myelin oligodendrocyte glycoprotein

CFA = Freund's complete adjuvant

NOD = Nonobese diabetic

dsDNA = Double-stranded DNA

REFERENCES

[1] Walker, L.S.K. and Abbas, A.K. (2002) *Nat. Rev. Immunol.*, 2(1), 11-19.

[2] Hammond, K.J.L. and Godfrey, D.I. (2002) *Tissue Antigens*, 59(5), 353-363.

[3] Wilson, S.B. and Delovitch, T.L. (2003) *Nat. Rev. Immunol.*, 3(3), 211-222.

[4] Porcelli, S.A. and Modlin, R.L. (1999) *Annu. Rev. Immunol.*, 17, 297-329.

[5] Kronenberg, M. and Gapin, L. (2002) *Nat. Rev. Immunol.*, 2(8), 557-568.

[6] Gumperz, J.E.; Miyake, S.; Yamamura, T. and Brenner, M.B. (2002) *J. Exp. Med.*, 195(5), 625-636.

[7] van Der Vliet, H.J.; Nishi, N.; de Gruijil, T.D.; von Blomberg, B.M.; van den Eertwegh, A.J.; Pinedo, H.M.; Giaccone, G. and Scheer, R.J. (2000) *Blood*, 95(7), 2440-2442.

[8] D'Andrea, A.; Goux, D.; De Lalla, C.; Koezuka, Y.; Montagna, D.; Moretta, A.; Dellabona, P.; Casorati, G. and Abrignani, S. (2000) *Eur. J. Immunol.*, 30(6), 1544-1550.

[9] Park, S.H.; Benlagha, K.; Lee, D.; Balish, E. and Bendelac, A. (2000) *Eur. J. Immunol.*, 30(2), 620-625.

[10] Kawano, T.; Cui, J.; Koezuka, Y.; Toura, I.; Kaneko, Y.; Motoki, K.; Ueno, H.; Nakagawa, R.; Sato, H.; Kondo, E.; Koseki, H. and Taniguchi, M. (1998) *Science*, 391(5343), 177-181.

[11] Brossay, L.; Chioda, M.; Burdin, N.; Koezuka, Y.; Casorati, G.; Dellabona, P. and Kronenberg, M. (1998) *J.Exp. Med.*, 188(8), 1521-1528.

[12] Spada, F.M.; Koezuka, Y. and Porcellim, S.A. (1998) *J. Exp. Med.*, 188(8), 1529-1534.

[13] Wu, D.Y.; Segal, N.H.; Sidobre, S.; Kronenberg, M. and Champan, P.B. (2003) *J. Exp. Med.*, 198(1), 173-181.

[14] Stetson, D.B.; Mohrs, M.; Reinhardt, R.L.; Baron, J.L.; Wang, Z-E.; Gapin, L.; Kroneneberg, M. and Locksley, R.M. (2003) *J. Exp. Med.*, 198(7), 1069-1076.

[15] Ansel, K.M.; Lee, D.U. and Rao, A. (2003) *Nat. Immunol.*, 4(7), 616-623.

[16] Oki, S.; Chiba, A.; Yamamura, T. and Miyake, S. (2004) *J. Clin. Invest.*, 113(11), 1631-1640.

[17] Shibasaki, F.; Price, ER.; Milan, D. and McKeon, F. (2000) *Nature*. 382(6589), 370-373.

[18] Owens, T.; Wekerle, H. and Antel, J. (2001) *Nat. Med.*, 7(2), 161-166.

[19] Chen, L.Z.; Hochwald, G.M.; Huang, C.; Dakin, G.; Tao, H. Cheng, C.; Simmons, W.J.; Dranoff, G. and Thorbecke, G.J. (1998) *Proc. Natl. Acad. Sci. USA*, 95(21), 12516-12521.

[20] Croxford, J.L.; Feldman, M.; Chernajovsky, Y. and Baker, D. (2001) *J. Immunol.*, 166(6), 4124-4130.

[21] Pal, E.; Tabira, T.; kawano, T.; Taniguchi, M.; Miyake, S. and Yamamura, T. (2001) *J. Immunol.*, 166(1), 662-668.

[22] Miyamoto, K.; Miyake, S. and Yamamura, T. (2000) *Nature*, 413(6855), 531-534.

[23] Jahng, A.W.; Maricic, I.; Pedersen, B.; Burdin, N. and Naidenko, O. (2001) *J. Exp. Med.*, 194(12), 1789-1799.

[24] Singh, A.K.; Wilson, M.T.; Hong, S.; Oliveres-Villagomez, D.; Du, C.; Stanic, A.K.; Joyce, S.; Siriam, S.; Koezka, Y. and Van Kaer, L. (2001) *J. Exp. Med.*, 194(12), 1801-1811.

[25] Furlan, R.; Bergami, A.; Cantarella, D.; Brambilla, E.; Taniguchi, M.; Dellabona, P.; Casorati, G. and Martino G. (2003) *Eur. J. Immunol.*, 33(7), 1830-1838.

[26] Yoshimoto, T.; Bendelac, A.; Hu-Li, J. and Pau, W.E. (1995) *Proc. Natl. Acad. Sci. USA*, 92(25), 11931-11934.

[27] Van Roon, J.A. G.; Lafeber, F.P.J.G. and Bijlsma, J.W.J. (2001) *Arthritis. Rheum.*, 44(1), 3-12.

[28] Chiba, A.; Oki, S.; Miyamoto, K.; Hashimoto, H.; Yamamura, T. and Miyake, S.(2001) *Arthritis. Rheum.*, 50(1), 305-313.

[29] Delovitch, T.L. and Singh, B. (1997) *Immunity*, 7(6), 727-738.

[30] Yoshida, K. and Kikutani, H. (2000) *Rev. Immunogenetics.*, 2(1), 140-146.

[31] Gombert, J-M, Herbelin, A.; Tancrede-Bohin, E.; Dy, M.; Carnaud, C. and Bach, J.-F. (1996) *Eur. J. Immunol.*, 26(12), 2989-2998.

[32] Shi, Fu-D.; Flodstrom, M.; Balasa, B.; Kim, S.H.; Van Gunst, K.; Strominger, J.L.; Wilson, B. and Sarvetnick N. (2001) *Proc. Natl. Acad. Sci. USA*, 98(12), 6777-6782.

[33] Wang, B.; Geng, Y.-B. and Wang, C.-R. (2001) *J. Exp. Med.*, 194(3), 313-319.

[34] Hammond, K.J.L.; Poulton, L.D.; almisano, L.J.; Silveira, P.A.; Godrey, D.I. and Bazter, A.G. (1998) *J. Exp. Med.*, 187(7), 1047-1056.

[35] Lehuen, A.; Lantz, O.; Beaudoin, L.; Laloux, V.; Carnaud, C.; Bendelac, A.; Bach, J.-F. and Monteriro, R.C. (1998) *J. Exp. Med.*, 188(9), 1831-1839.

[36] Sharif, S.; Arreaza, G.A.; Zucker, P.; Mi, Q-S.; Sondhi, J.; Naidenko, O.V.; Kronenberg, M.; Koezuka, Y. and Delovitch, T.L.; Gombert, J-M.; Leite-de-Moraes, M.; Gouarin, C.; Zhu, R.; Hameg, A.; Nakayama, T.; Taniguchi, M.; Lepault, F.; Lehuen, A.; Bach, J-F. and Herbelin A. (2001) *Nat. Med.*, 7(9), 1057-1062.

[37] Hong, S.; Wilson, M.T.; Serizawa, I.; Wu, L.; Singh, N.; Naidenko, O.V.; Miura, T.; Haba, T.; Scherer, D.C.; Wei, J.; Kronenberg, M.; Koezuka, Y. and Van Kaer, L. (2001) *Nat. Med.*, 7(9), 1052-1056.

[38] Naumov, Y.N.; Bahjat, K.S.; Gausling, R.; Abraham, R.; Exley, M.A.; Koezuka, Y.; Balk, S.B.; Strominger, J.L.; Clare-Salzer, M. and Wilson, S.B. (2001) *Proc. Natl. Acad. Sci. USA*, 98(24), 13838-13843.

[39] Mieza, M.A.; Itoh, T.; Cui, J.Q.; Makino, Y.; Kawano, T.; Tsuchida, K.; Koike, T.; Shirai, T.; Yagita, H.; Matsuzawa, A.; Koseki H. and Taniguchi, M. (1996) *J. Immunol.*, 156(10), 4035-4040.

[40] Zeng, D.; Liu, Y.; Sidobre, S.; Kronenberg, M. and Strober, S. (2003) *J. Clin. Invest.*, 112(8), 1211-1222.

[41] Yang, J.Q.; Singh, A.K.; Wilson, M.T.; Satoh, M.; Stanic, A.K.; Par, J.-J.; Hong, S.; Gadola, S.D.; Mizutani, A.; Kakumanu, S.R.; Reeves, W.; Cerundolo, V.; Joyce, S.; Van Kaer, L. and Singh, R.R. (2003) *J. Immunol.*, 171(4), 2142-2153.

[42] Yang, J-Q.; Saxena, V.; Xu, H.; Van Kaer, L.; Wang, C.-R. and Singh, R.R. (2003) *J. Immunol.*, 171(8), 4439-4446.

[43] Illes, Z.; Kondo, T.; Newcombe, J.; Oka, N.; Tabira, T. and Yamamura, T. (2000) *J. Immunol.*, 164(8), 4375-4381.

[44] Van der Vliet, H.J.J.; von Blomberg, B.M.E.; Nishi, N.; Reijm, M.; Voskuyl, A.E.; van Bodegraven, A.; Polman, C.H.; Rustemeyer, T.;Lips, P.; van den Eertwegh, A.J.M.; Giaccone, G.; Scheper, R.J. and Pinedo, H.M. (2001) *Clin. Immunol.*, **100**(2), 144-148.

[45] Araki, M.; Kondo, T.; Gumperz, J.E.; Brenner, M.B.; Miyake, S. and Yamamura, T. (2003) *Int. Immunol.*, **15**(2), 279-288.

[46] Gausling, R.; Trollmo, C. and Hafler, D.A. (2001) *Clin. Immunol.*, 98(1), 11-17.

[47] Wilson, S.B.; Kent, S.C.; Patton, K.T.; Orban, T.; Jackdon, R.A.; Exley, M.; Porcelli, S.; Schatz, D.A.; Atkinson, M.A.; Balk, S.P.; Strominger, J.L. and Hafler, D.A. (1998) *Nature*, **391**(6663), 177-181.

[48] Kukreja, A.; Cost, G.; Marker, J.; Zhang, C, Sun, Z.; Lin-Su, K.; Ten, S.; Sanz, M, Exley, M.; Wilson, B, Porcelli, S.; Maclaren, N. (2002) *J. Clin. Invest.*, **109**(1), 131-140.

[49] Lee, P.T.; Putnam, A.; Benlagha, K.; Teyton, L.; Gottlieb, P.A. and Bendelac, A. (2002) *J. Clin. Invest.*, **110**(6), 793-800.

[50] Oikawa, Y.; Shimada, A.; Yamada, S.; Motohashi, Y.; Nakagawa Y.; Irie, J.; Maruyama, T. and Saruta, T. (2002) *Diabet. Care* **25**(10), 1818-1823.

[51] Sumida, T.; Sakamoto, A.; Murata, H.; Makino, Y.; Takahashi, H. Yoshida, H.; Nishioka, K.; Iwamoto, I. and Taniguchi, M. (1995) *J Exp. Med.*, **182**(4), 1163-1168.

[52] Maeda, T.; Keino, H.; Asahara, M.; Taniguchi, M.; Nishioka, K and Sumida, T. (1999) *Rheumatology*, **38**(2), 186-188.

[53] Oishi, Y.; Sumida, T.; Sakamoto, A.; Kita, Y.; Kurasawa, K. Nawata, Y.; Takabayashi, K.; Takahashi, H.; Yoshida, S.; Tanigu chi, M.; Saito, Y. and Iwamoto, I. (2001) *J. Rhuematol.*, **28**(2), 275 283.

[54] Sumida, T.; Maeda, T.; Taniguchi, M.; Nishioka, K. and Stohl, W (1998) *Lupus*, **7**(8), 565-568.

[55] Kojo, S.; Adachi, Y.; Keino, H.; Taniguchi, M. and Sumida, T (2001) *Arthritis. Rheum.*, **44**(5), 1127-1138.

[56] Mizuno, M.; Masumura, M.; Tomi, C.; Chiba, A.; Oki, S.; Yama mura, T.; Miyake, S. (2004) *J. Autoimmune*, **23**, 293-300.

Journal of Neurochemistry, 2005, **93**, 63–71 doi:10.1111/j.1471-4159.2004.02994.x

Selective gene silencing of rat ATP-binding cassette G2 transporter in an *in vitro* blood–brain barrier model by short interfering RNA

Satoko Hori,*,†,¶ Sumio Ohtsuki,*,†,¶ Masashi Ichinowatari,* Takanori Yokota,‡ Takashi Kanda‡ and Tetsuya Terasaki*,†,¶

**Department of Molecular Biopharmacy and Genetics, Graduate School of Pharmaceutical Sciences, Tohoku University, Sendai, Japan*

†New Industry Creation Hatchery Center, Tohoku University, Sendai, Japan

¶CREST and SORST of the Japan Science and Technology Agency (JST), Japan

‡Department of Neurology and Neurological Science, Graduate School of Medicine, Tokyo Medical and Dental University, Tokyo, Japan

Abstract

The aim of the present study was to specifically silence the rat ATP-binding cassette transporter G2 (rABCG2) gene in brain capillary endothelial cells by transfection of short interfering RNA (siRNA). Four different siRNAs designed to target rABCG2 were each transfected into HEK293 cells with myc-tagged rABCG2 cDNA. Quantitative real-time PCR and western blot analyses revealed that three of the siRNAs were able to reduce exogenous rABCG2 mRNA and protein levels in HEK293 cells. Moreover, rABCG2-mediated mitoxantrone efflux transport was suppressed by the introduction of these three siRNAs into HEK293 cells. In contrast, the other siRNA and non-specific control siRNA did not significantly affect the mRNA expression, the protein level or the transport activity. Endogenous rABCG2 mRNA and protein expression in a conditionally immortalized rat brain capillary endothelial cell line (TR-BBB13) was suppressed by the most potent siRNA among the four siRNAs tested. Furthermore, this siRNA did not affect the mRNA levels of other ABC transporters, such as ABCB1, ABCC1 and ABCG1, and the protein level of ABCB1 in TR-BBB13 cells, suggesting that it can selectively silence rABCG2 at the blood–brain barrier. This should be a useful and novel strategy for clarifying the contribution of rABCG2 to brain-to-blood transport of substrate drugs and endogenous compounds across the blood–brain barrier.

Keywords: ABC transporter, ATP-binding cassette transporter G2, 17β-estradiol, blood–brain barrier, *in vitro* blood–brain barrier model, short interfering RNA.

J. Neurochem. (2005) **93**, 63–71.

The blood–brain barrier (BBB), which is formed by the tight intercellular junctions of brain capillary endothelial cells (BCECs), strictly regulates the transfer of substances between the circulating blood and the brain (Terasaki and Hosoya 1999; Hosoya *et al.* 2002). Therefore, the molecular mechanisms of efflux transport from the brain have important implications for drug delivery and CNS homeostasis.

ABCG2 (BCRP/MXR/ABCP1) is an ATP-binding cassette (ABC) transporter localized on the luminal side of brain capillaries in humans (Cooray *et al.* 2002) and rats (Hori *et al.* 2004), and transports a diverse array of compounds out of the cells (Allen and Schinkel 2002). Therefore, ABCG2 present in BCECs may act to restrict the penetration of xenobiotics into the brain and to pump out potential toxins or metabolites from the brain. ABCG2 transports sulfated conjugates of drugs and sterols (Suzuki *et al.* 2003), whereas p-glycoprotein (P-gp), a well-characterized efflux transporter at the BBB, preferentially transports hydrophobic

Received May 10, 2004; revised manuscript received November 16, 2004; accepted November 17, 2004.

Address correspondence and reprint requests to Tetsuya Terasaki, Department of Molecular Biopharmacy and Genetics, Graduate School of Pharmaceutical Sciences, Tohoku University, Aoba, Aramaki, Aoba-ku, Sendai 980–8578, Japan. E-mail: terasaki@mail.pharm.tohoku.ac.jp

Abbreviations used: ABC, ATP-binding cassette; BBB, blood–brain barrier; BCEC, brain capillary endothelial cell; DHEAS, dehydroepiandrosterone sulfate; NC, non-specific control; PMSF, phenylmethylsulphonyl fluoride; SDS–PAGE, sodium dodecyl sulfate polyacrylamide gel electrophoresis; siRNA, short interfering RNA; TR-BBB, conditionally immortalized brain capillary endothelial cell line.

compounds. Therefore, ABCG2 may have a distinct role in efflux transport at the BBB.

Several ABC transporters and organic anion transporters are expressed at the abluminal and/or luminal membrane of the BBB as well as ABCG2 (Gao *et al.* 1999; Virgintino *et al.* 2002; Mori *et al.* 2003). Clarifying the transport properties and the contribution of each transporter at the BBB is an important issue for understanding the physiological roles of these molecules. However, the substrate and inhibitor specificities of these transporters sometimes overlap. For example, dehydroepiandrosterone sulfate (DHEAS) is transported from brain to the circulating blood across the BBB via organic anion transporting polypeptide 2 (Asaba *et al.* 2000), while other transporters at the BBB, such as ABCG2 and ABCC4 (Zhang *et al.* 2000; Cooray *et al.* 2002; Hori *et al.* 2004), also accept DHEAS as a substrate (Suzuki *et al.* 2003; Zelcer *et al.* 2003).

Three effective inhibitors of ABCG2 have been described thus far. GF120918 was developed as a P-gp (ABCB1) inhibitor (Hyafil *et al.* 1993), but a later study found that it also inhibits ABCG2 (de Bruin *et al.* 1999). Such a dual-specificity inhibitor is unsuitable for clarifying the distinct transport activity of each transporter. Fumitoremorgin C and Ko143 are potent and selective inhibitors for ABCG2, being much less active towards P-gp and ABCCs (Rabindran *et al.* 2000; Allen *et al.* 2002). Nevertheless, the specificity of these inhibitors is concentration-dependent, and an influence of these two inhibitors on unidentified transporters at the BBB cannot be ruled out.

RNA interference is a conserved biological response to double-stranded RNA, which results in sequence-specific gene silencing (Hannon 2002). In mammalian cell cultures, double-stranded RNA-mediated interference with gene expression has also been accomplished by transfection of synthetic RNA oligonucleotides composed of 21 or 22 base pairs (short interfering RNA, siRNA; Elbashir *et al.* 2002). Sequence-specific silencing of transporter genes using siRNA should make it possible to evaluate properly the transport properties of a targeted transporter at the BBB.

Conditionally immortalized BCEC lines are useful *in vitro* BBB models which retain the *in vivo* transport properties towards various compounds (Hosoya *et al.* 2000a, 2000b; Terasaki *et al.* 2003). Endothelial cells are generally resistant to the introduction of exogenous DNA, and molecular analysis of endothelial cells has been hampered by the difficulty of transiently transfecting genes with high efficiency. Therefore, siRNA-induced specific knockdown of target transporter genes in BCECs should allow us to improve our understanding of the physiological and pharmacological functions of the efflux transport systems at the BBB.

The purpose of this study was therefore to specifically silence rABCG2 gene by the introduction of siRNA into BCECs, in order to clarify the role of ABCG2 at the BBB.

Materials and methods

Reagents

Endothelial cell growth factor (ECGF) was purchased from Boehringer Mannheim (Mannheim, Germany). Benzylpenicillin potassium and streptomycin sulfate were purchased from Wako Pure Chemical Industries (Osaka, Japan). Non-specific Control Duplex XI (NC siRNA; Dharmacon, Lafayette, CO, USA) is claimed by the manufacturer to show no RNAi effect, and its target sequence is 5′-NNATAGATAAGCAAGCCTTAC-3′. No rat gene sequences with homology to NC siRNA were found by Blast search. β-Actin siRNA was purchased from Qiagen (Tokyo, Japan); its target sequence is 5′-AATGAAGATCAAGATCATTGC-3′. The sequence of β-actin siRNA is identical at 20 bp out of 21 bp with the corresponding sequence of rat β-actin (the underlined base in the sequence of β-actin siRNA is changed to 'C' in that of rat β-actin). All other chemicals were commercial products of analytical grade.

siRNA preparation

Four different siRNA duplexes were designed based on the coding sequence of rABCG2 cDNA (GenBank accession number AB105817). All 21-nucleotides (nt) siRNAs contained 3′-dTdT extensions and their GC contents were less than 70%. The sequences, positions and GC contents of siRNA targeting rat ABCG2 are shown in Table 1. All of the siRNA duplexes were

Table 1 Sequences of rABCG2 short interfering RNAs (siRNAs)

Number of rABCG2 siRNA	Sequences (upper, sense; lower, antisense)	Positions*/GC (%)
01	5′-CAGAGAAACAAGAACGGCCdTdT dTdTGUCUCUUUGUUCUUGCCGG-5′	95–113/52.6%
02	5′-UGUGCUAAGUUUUCAUCACdTdT dTdTACACGAUUCAAAAGUAGUG-5′	160–178/36.8%
03	5′-CCCUGACAGUGAGAGAAAAdTdT dTdTGGGACUGUCACUCUCUUUU-5′	450–468/47.4%
04	5′-GCAAACAAGACAGAAGAGCdTdT dTdTCGUUUGUUCUGUCUUCUCG-5′	998–1016/47.4%

*GenBank accession number AB105817.

chemically synthesized and HPLC-purified by Proligo (La Jolla, CA, USA).

Cell culture

HEK293 cells (American Type Culture Collection, Rockville, MD, USA) were grown in Dulbecco's modified Eagle's medium (DMEM, Nissui Pharmaceutical, Tokyo, Japan) supplemented with 20 mM sodium bicarbonate, 100 U/mL benzylpenicillin potassium, 100 μg/mL streptomycin sulfate and 10% fetal bovine serum (Moregate, Bulimba, Australia; culture-medium A) at 37°C in a humidified atmosphere of 95% air and 5% CO_2. TR-BBB13 cells are a conditionally immortalized BCEC cell line (Hosoya *et al.* 2000a) that has been used as an *in vitro* BBB model (Terasaki *et al.* 2003). TR-BBB13 cells were grown in culture-medium A with 15 ng/mL ECGF. The cells were maintained at 33°C, which is a permissive temperature at which temperature-sensitive SV40 large T-antigen is activated, in a humidified atomosphere of 95% air and 5% CO_2.

Transfection of siRNA into HEK293 cells or TR-BBB13 cells

HEK293 cells were plated in six-well plates at 4×10^5 cells/well, grown for 24 h then transfected with 3 μg of rABCG2 siRNA-01, rABCG2 siRNA-02, rABCG2 siRNA-03, rABCG2 siRNA-04 or NC siRNA using Lipofectamine 2000 and OPTI-MEM I reduced serum medium (Invitrogen, Carlsbad, CA, USA). In some experiments, 1 μg of myc-tagged rABCG2 cDNA (pCMV-Tag3A/rABCG2 (Hori *et al.* 2004)) or a control plasmid (pCMV-Tag3A, Stratagene, La Jolla, CA, USA) was co-transfected into HEK293 cells simultaneously with siRNA. The mRNA expression and the transport activity were examined at 48 h after the transfection. The protein expression was examined at 24, 48 and 72 h after the transfection.

For quantitative real-time PCR analysis, TR-BBB13 cells were plated in six-well plates at 4×10^5 cells/well, grown for 24 h at 33°C then transfected with 4 μg of rABCG2 siRNA-03, β-actin siRNA or NC siRNA using Lipofectamine 2000 and OPTI-MEM I reduced serum medium (Invitrogen). At 24 h after siRNA transfection, TR-BBB13 cells were treated with or without 100 nM 17β-estradiol. Culture was continued for a further 24 h at 33°C. For western blot analysis, TR-BBB13 cells were plated in six-well plates at 4×10^5 cells/well, grown for 24 h at 33°C then transfected with 4 μg of rABCG2 siRNA-03 or NC siRNA using Lipofectamine 2000 and OPTI-MEM I reduced serum medium (Invitrogen). The protein expression was examined at 36 h after the transfection.

Quantitative real-time PCR analysis

Total RNA was extracted from HEK293 cells or TR-BBB13 cells with an RNeasy kit (Qiagen) according to the manufacturer's protocol. RNA integrity was checked by electrophoresis on an agarose gel. Single-stranded cDNA was prepared from 1 μg of total RNA by RT (ReverTraAce, Toyobo, Osaka, Japan) using oligo dT primer. Quantitative real-time PCR analysis was performed using an ABI PRISM 7700 sequence detector system (PE Applied Biosystems, Foster City, CA, USA) with 2 × SYBR Green PCR Master Mix (PE Applied Biosystems) according to the manufacturer's protocol. To quantify the amount of specific mRNA in the samples, standards for each run were prepared using pGEM-T Easy Vector containing ABCG2, ABCB1, ABCC1, ABCG1, β-actin or GAPDH (dilution ranging from 0.1 fg/μL to 1 ng/μL). The standard curves of each gene were obtained by linear regression between the logarithm of the standards of each gene and the corresponding threshold cycle (Ct) values. The Ct value indicates the cycle number at which the reaction begins to be exponential. All the plots showed high linearity, and the Ct values of all samples were within the range of the standard plots. The ABCG2, ABCB1, ABCC1 or ABCG1 mRNA levels were normalized relative to the β-actin mRNA level. The β-actin mRNA level was normalized relative to the GAPDH mRNA level. In Fig. 1, each rABCG2 mRNA level is indicated as a percentage of the mean of those in HEK293 cells co-transfected with NC siRNA and rABCG2 cDNA ($n = 3$; open column, NC+). In Fig. 4, each mRNA level is indicated as a percentage of the mean of mRNA levels in TR-BBB13 cells treated with non-siRNA (–) and 17β-estradiol (E2; $n = 3$; the leftmost column). The control lacking the RT enzyme was assayed in parallel to monitor any possible genomic contamination. The PCR was run for 40 cycles of 95°C for 30 s, 60°C for 1 min, and 72°C for 1 min after pre-incubation at 95°C for 10 min, using specific primers. The sequences of primers were as follows: sense primer 5′-CAATGGGATCATGAAACC-TG-3′, antisense primer 5′-GAGGCTGATGAATGGAGAA-3′ for ABCG2; sense primer 5′-ACAGAAACAGAGGATCGC-3′ and antisense primer 5′-CGTCTTGATCATGTGGCC-3′ for ABCB1/mdr1a; sense primer 5′-CTGGCTTGGTGTGAACTGAT-3′ and antisense primer 5′-AGGCTCTGGCTTGGCTCTAT-3′ for ABCC1; sense primer 5′-TGCCCGCCGGGTTGAAACTGTTC-3′ and antisense primer 5′-ACTGTCTGCATTGCGTTGCATTGC-3′ for ABCG1; sense primer 5′-TTTGAGACCTTCAACACCCC-3′ and

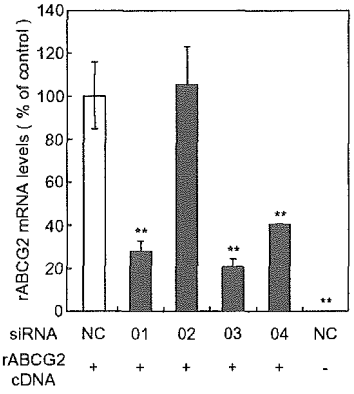

Fig. 1 Effects of rABCG2 siRNAs on the exogenous rABCG2 mRNA level in HEK293 cells co-transfected with myc-tagged rABCG2 cDNA. HEK293 cells were transfected with siRNAs (rABCG2 siRNA-01, rABCG2 siRNA-02, rABCG2 siRNA-03 and rABCG2 siRNA-04 (01, 02, 03 and 04) or non-specific control (NC) siRNA) with (+) or without (–) co-transfection of myc-tagged rABCG2 cDNA. At 48 h after transfection, the cells were collected for quantitative real-time PCR analysis. The sequences of rABCG2 siRNAs are shown in Table 1. Each column represents the mean ± SEM ($n = 3$). The rABCG2 mRNA level was normalized relative to the β-actin mRNA level. Each rABCG2 mRNA level is shown as percentage of the mean of the rABCG2 mRNA level in the NC siRNA-treated HEK293 cells cotransfected with myc-tagged rABCG2 cDNA (NC+). $^{**}p < 0.01$, significantly different from the NC+.

antisense primer 5′-ATAGCTCTTCTCCAGGGAGG-3′ for β-actin; sense primer 5′-TGATGACATCAAGAAGGTGGTGAAG-3′ and antisense primer 5′-TCCTTGGAGGCCATGTAGGCCAT-3′ for *GAPDH*.

Western blot analysis

HEK293 cells were lysed with lysis buffer containing 10 mM Tris–HCl (pH 7.4), 1 mM EDTA, 150 mM NaCl, 4% CHAPS, 1 mM phenylmethylsulfonyl fluoride, and a protease-inhibitor cocktail (Sigma Chemical Co., St Louis, MO, USA). The lysate was centrifuged at 15 000 *g* for 30 min and the supernatants were collected. TR-BBB13 cells were homogenized by mean of the nitrogen cavitation technique (800 psi, 15 min, 4°C) in buffer containing 10 mM HEPES-NaOH (pH 7.4), 250 mM sucrose, 1 mM EDTA, 1 mM phenylmethylsulphonyl fluoride (PMSF). The homogenized samples were centrifuged at 10 000 *g* for 10 min and the supernatants were collected. These supernatants were centrifuged at 100 000 *g* for 1 h, and a crude membrane fraction was obtained from the pellets. The pellets were suspended in lysis buffer. The protein concentration of samples was measured by the Bradford method using Bio-Rad Protein Assay reagent (Bio-Rad, Hercules, CA, USA). Protein samples (HEK293 cells, 12 μg; TR-BBB13 cells, 40 μg (for rABCG2) or 20 μg (for Na^+,K^+-ATPase and ABCB1) per lane) were resolved by 7.5% sodium dodecyl sulfate polyacrylamide gel electrophoresis (SDS–PAGE; Bio-Rad) and subsequently electrotransferred to nitrocellulose membranes. Membranes were treated with blocking buffer (4% skimmed milk in 25 mM Tris–HCl (pH 8.0), 125 mM NaCl, 0.1% Tween-20 for 2 h at 20°C and incubated with anti-c-myc antibody (0.1 μg/mL; Bethyl Laboratories Inc., Montgomery, TX, USA), anti-β-actin antibody (1 : 2000; Sigma), anti-Na^+,K^+-ATPase antibody (0.1 μg/mL; Upstate Biotechnology, Lake Placid, NY, USA), anti-ABCB1 antibody (C219) (1 : 100; Signet, Dedham, MA, USA), or anti-ABCG2 antibody (G2-Ab1) (1.0 μg/mL) (Hori *et al.* 2004) as the primary antibody at 4°C for 16 h after blocking. The membranes were washed three times with blocking buffer and incubated with horseradish peroxidase-conjugated second antibody. The bands were visualized with an enhanced chemiluminescence kit (SuperSignal; Pierce, Rockford, IL, USA). The relative densities of the bands were measured using NIH image software (National Institutes of Health, Bethesda, MD, USA).

Transport assay

For transport studies, HEK293 cells were incubated for 1 h at 37°C in a medium containing 20 μM mitoxantrone. The cells were then washed in ice-cold phosphate-buffered saline and placed on ice until measurement. Relative cellular accumulation of mitoxantrone was determined by flow cytometry with a 635 nm red diode laser and 661 nm bandpass filter (FACs Calibur, BD Biosciences, Lexington, KY, USA). A total of 20 000 events were collected. Debris was eliminated by gating on forward versus side scatter. The mean channel number for each histogram was used as a measure of drug fluorescence for calculation.

Data analysis

Unless otherwise indicated, all data represent the mean ± SEM. An unpaired, two-tailed Student's *t*-test was used to determine the significance of differences between two group means. One-way ANOVA followed by the modified Fisher's least-squares difference method was used to assess the statistical significance of differences among means of more than two groups.

Results

Silencing of exogenous rABCG2 gene in HEK293 cells

To determine the effects of four different siRNAs (rABCG2 siRNA-01, rABCG2 siRNA-02, rABCG2 siRNA-03 and rABCG2 siRNA-04; Table 1) on rABCG2 gene expression, quantitative real-time PCR analysis was performed using HEK293 cells co-transfected with myc-tagged rABCG2 cDNA. After treatment with rABCG2 siRNA-01, rABCG2 siRNA-03 or rABCG2 siRNA-04 for 48 h, the rABCG2 mRNA levels were suppressed in rABCG2-transfected HEK293 cells by 71.8%, 78.8% or 54.7%, respectively (01+, 03+ and 04+, Fig. 1), compared with those in cells treated with non-specific control (NC) siRNA (NC+, Fig. 1). In contrast, treatment with rABCG2 siRNA-02 had no significant effect on the rABCG2 mRNA level (02+, Fig. 1).

Effects of siRNAs on rABCG2 protein level in HEK293 cells

To clarify whether rABCG2 protein was reduced concomitantly with the suppression of rABCG2 mRNA, the level of exogenous rABCG2 protein was examined by western blot analysis. The protein was detected using anti-c-myc antibody, as rABCG2 protein was fused with the myc epitope. Myc tagged-rABCG2 proteins were detected at 80 kDa in HEK293 cells co-transfected with NC siRNA and myc-tagged rABCG2 cDNA (NC+, Fig. 2a), while no band was detected in HEK293 cells co-transfected with NC siRNA and the vector alone (i.e. without the myc-tagged rABCG2 cDNA insert) (NC−, Fig. 2a). rABCG2 siRNA-01, rABCG2 siRNA-03 and rABCG2 siRNA-04 each reduced the level of rABCG2 protein in HEK293 cells co-transfected with myc-tagged rABCG2 cDNA (01+, 03+ and 04+, Fig. 2a). rABCG2 siRNA-03 was the most effective (03+, Fig. 2a), and it reduced the relative density of the bands by 99.7 ± 0.1% (mean ± SEM; $n = 3$) compared with NC siRNA. In contrast, the rABCG2 protein level was not affected by rABCG2 siRNA-02 (02+, Fig. 2a). The level of β-actin protein was unchanged by any of the rABCG2 siRNAs (Fig. 2a). As shown in Figs 2(b and c), western blot analysis at 24 h and 72 h after transfection clearly demonstrated that co-transfection of rABCG2 siRNA-03, but not NC siRNA, significantly reduced the level of rABCG2 protein.

Effects of rABCG2 siRNAs on mitoxantrone efflux transport in rABCG2 cDNA-transfected HEK293 cells

Mean fluorescence intensity of mitoxantrone was significantly reduced in HEK293 cells following co-transfection with NC siRNA and myc-tagged rABCG2 cDNA (NC+, Fig. 3a) compared with NC siRNA alone (NC−, Fig. 3a). The proportion of transiently rABCG2 cDNA-transfected cells was 25.7 ± 0.4% (mean ± SEM; $n = 3$; gated area, Fig. 3b). rABCG2 siRNA-01, rABCG2 siRNA-03 and rABCG2 siRNA-04 significantly increased the mean fluorescence intensity of mitoxantrone (01+, 03+ and 04+, Fig. 3a), and indeed, rABCG2 siRNA-03 completely reversed the reduction of the mitoxantrone level. Representative histogram and dot plots showed that the population of rABCG2-transfected cells almost completely

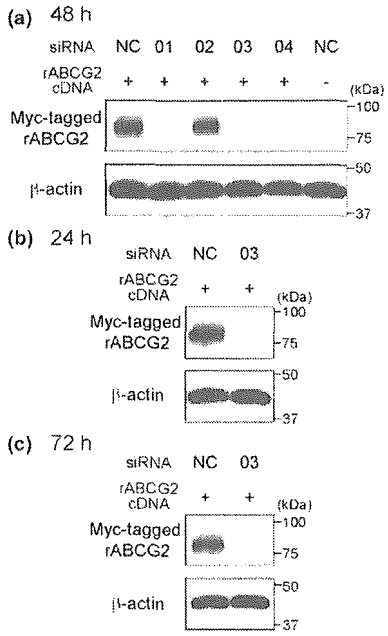

Fig. 2 Effects of rABCG2 siRNAs on exogenous rABCG2 protein in HEK293 cells co-transfected with myc-tagged rABCG2 cDNA. HEK293 cells were transfected with siRNAs (rABCG2 siRNA-01, rABCG2 siRNA-02, rABCG2 siRNA-03 and rABCG2 siRNA-04 (01, 02, 03 and 04) or non-specific control (NC) siRNA) with (+) or without (–) co-transfection of myc-tagged rABCG2 cDNA. The sequence of rABCG2 siRNAs are shown in Table 1. At 48 h (a), 24 h (b) or 72 h (c) after transfection, the cells were collected for western blot analysis using anti-c-myc and anti-β-actin antibodies. Typical results from repeated experiments are shown.

overlapped with that of non-transfected cells (03+, Fig. 3b). In contrast, rABCG2 siRNA-02 had no significant effect on the mean fluorescence intensity of mitoxantrone in HEK293 cells (02+, Fig. 3a).

Selective inhibition of endogenous rABCG2 gene in a conditionally immortalized BCEC line (TR-BBB13) by siRNA

rABCG2 siRNA-03, which is the most potent siRNA for attenuating rABCG2 function, was used to suppress endogenous rABCG2 expression in TR-BBB13 cells. At 24 h after siRNA transfection, TR-BBB13 cells were treated with 17β-estradiol, which has been reported to induce ABCG2 mRNA expression in cancer cells (Ee *et al.* 2004), or not treated. In the absence of 17β-estradiol, the rABCG2 mRNA level was reduced by 42.2% by transfection of rABCG2 siRNA-03 into TR-BBB13 cells (G2-03), whereas transfection of NC siRNA had no effect (NC)[E_2(–), Fig. 4a]. The rABCG2 mRNA level was significantly induced in non-siRNA-transfected TR-BBB13 cells following treatment with 17β-estradiol (open columns, Fig. 4a). The rABCG2 mRNA level was reduced by 75.7% by transfection of rABCG2 siRNA-03 into TR-BBB13 cells in the presence of 17β-estradiol (G2-03)[E_2(+), Fig. 4a]. In contrast, the transfection of NC siRNA did not affect the rABCG2 mRNA level in TR-BBB13 cells (NC)[E_2(+), Fig. 4a]. Treatment with siRNA targeted to β-actin decreased the β-actin mRNA level by 57.9 ± 2.2% (mean ± SEM; $n = 3$) in TR-BBB13 cells, supporting the view that siRNA was successfully transfected into TR-BBB13 cells.

To confirm the selectivity of the inhibitory effects of siRNA, the expression levels of other ABC transporters expressed in BCECs were examined. rABCG2 siRNA-03 did not significantly affect the ABCB1, ABCC1 and ABCG1 mRNA levels in TR-BBB13 cells in either the presence or absence of 17β-estradiol (Figs 4b–d). Following the 17β-estradiol treatment, the ABCB1 mRNA level was increased in TR-BBB13 cells (Fig. 4b), whereas the ABCC1 mRNA level showed a tendency to decrease (Fig. 4c), and the ABCG1 mRNA level was unchanged (Fig. 4d).

Suppression of endogenous rABCG2 protein expression in TR-BBB13 cells by siRNA

The rABCG2 protein expression was suppressed by transfection of rABCG2 siRNA-03 into TR-BBB13 cells (G2-03) compared with untransfected (–) and NC siRNA-transfected (NC) TR-BBB13 cells (Fig. 5a, upper panel). The expression of ABCB1 protein and Na^+,K^+-ATPase protein, used as a standard, was not changed by any of the treatment conditions (Fig. 5a, middle and lower panel, respectively). As shown in Fig. 5(b), the density ratio of rABCG2 to Na^+,K^+-ATPase density was significantly decreased by 62.1% by transfection of rABCG2 siRNA-03 into TR-BBB13 cells (G2-03) compared with untransfected TR-BBB13 cells (–).

Discussion

The present study demonstrated that introduction of any of three rABCG2 siRNAs efficiently decreased the expression of rABCG2 and suppressed the apparent efflux function of mitoxantrone, a substrate drug of rABCG2. Moreover, rABCG2 siRNA selectively suppressed the mRNA and protein expression of rABCG2 in a conditionally immortalized brain capillary endothelial cell line (TR-BBB), an *in vitro* BBB model.

Three of the siRNAs designed to target the rABCG2 gene induced sequence-specific suppression of the expression and function of the rABCG2 transporter (Figs 1–3). None of the siRNAs affected the β-actin protein levels (Fig. 2). This is the first evidence that rABCG2 function can be suppressed by siRNA-induced RNA interference. The differences in efficacy among these three siRNAs could be due to altered ability to silence the rABCG2 gene rather than altered transfection efficiency, because rABCG2 siRNA was present in about 900-fold molar excess over rABCG2-expression plasmid (the amount/length of the rABCG2 siRNA and the plasmid was 3 μg/21 bp and 1 μg/about 6300 bp, respectively). The protein expression and the transport activity of rABCG2 were completely suppressed at 48 h after rABCG2 siRNA-03 transfection (Figs 2 and 3), while reduction of the mRNA expression was around 80% (Fig. 1). This apparent difference may be because the protein level was below the detection threshold of western blot analysis, and below the level required for exerting its function. The expression of

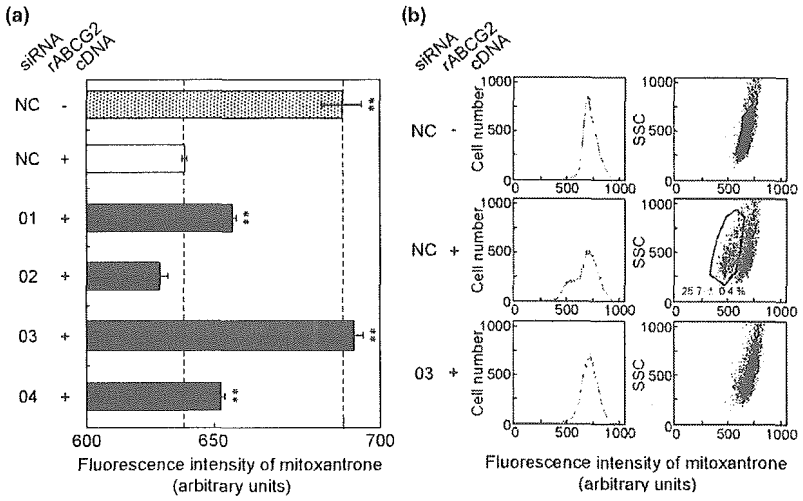

Fig. 3 Effects of rABCG2 siRNAs on mitoxantrone efflux transport in HEK293 cells co-transfected with myc-tagged rABCG2 cDNA. (a) HEK293 cells were transfected with siRNAs (rABCG2 siRNA-01, rABCG2 siRNA-02, rABCG2 siRNA-03 and rABCG2 siRNA-04 (01, 02, 03 and 04) or non-specific control (NC) siRNA) with (+) or without (–) cotransfection of myc-tagged rABCG2 cDNA. The sequences of rABCG2 siRNAs are shown in Table 1. At 48 h after transfection, the cells were incubated with 20 μM mitoxantrone for 1 h at 37°C. Mitoxantrone fluorescence in arbitrary units was determined by flow cytometry with a 635 nm red diode laser and 661 nm bandpass filter. Each column represents the mean ± SEM ($n = 3$). $^{**}p < 0.01$, significantly different from the NC siRNA-treated HEK293 cells co-transfected with myc-tagged rABCG2 cDNA (NC +). (b) Representative histogram plot and dot plot of HEK293 cells transfected with siRNAs [NC siRNA or rABCG2 siRNA-03 (03)] with (+) or without (–) myc-tagged rABCG2 cDNA, showing the mitoxantrone fluorescence vs. cell number and side scattered light (SSC), respectively. The gated cell population (solid line) identified the mitoxantrone-effluxing cells. The number shown is the proportion of total rABCG2-transfected cells contained in the gated cell population (mean ± SEM; $n = 3$).

exogenous rABCG2 protein was also completely suppressed at 24 h and 72 h after rABCG2 siRNA-03 transfection (Fig. 2), indicating that this siRNA remains effective at least from 24 h to 72 h. The sequence of rABCG2 siRNA-03 is 100% identical with the corresponding sequence of mouse ABCG2 (GenBank accession number NM011920). Therefore, this siRNA could be also effective for suppressing the function of mouse ABCG2.

The sequence locations of the effective rABCG2 siRNA-01, rABCG2 siRNA-03 and rABCG2 siRNA-04 (Table 1) were not limited to within 100-nucleotides downstream from the first ATG in contrast to the previous siRNA design (Elbashir *et al.* 2002). This result is in agreement with the recent report indicating that the major determinant of siRNA activity is the target sequence itself, rather than its location (Yoshinari *et al.* 2004). Recently, eight criteria for rational siRNA design for RNA interference were proposed (Reynolds *et al.* 2004). Indeed, the most effective rABCG2 siRNA (rABCG2 siRNA-03) satisfied as many as six of the criteria. For instance, this siRNA has moderate to low G/C content (30–52%), low internal stability of the sense 3′-end (at least three A/U bases at 15–19 nt) and a lack of internal repeats. Moreover, rABCG2 siRNA-03 has 'A' and 'U' at positions 19 and 10, respectively. It has been reported that these sequence-related criteria had a strong impact on improved selection of highly potent siRNAs (the increase in the probability of selecting siRNAs which induce more than 95% gene silencing was 7.2% and 12.8% for A19 and U10, respectively; Reynolds *et al.* 2004).

The present study has demonstrated that the delivery of siRNA suppresses rABCG2 mRNA and protein expression in TR-BBB13 cells (Figs 4a and 5), which are an *in vitro* BBB model expressing functional rABCG2 (Hori *et al.* 2004). There have been reports that the protein and function of targeted transporters were suppressed concomitantly with silencing of the corresponding genes (Wu *et al.* 2003; Nabokina *et al.* 2004; Said *et al.* 2004). Indeed, the endogenous rABCG2 protein level was suppressed in TR-BBB13 cells concomitantly with its gene silencing. rABCG2 siRNA-03 presumably suppresses transport activity of endogenous rABCG2 in TR-BBB13 cells by the reduction of rABCG2 protein level. The rABCG2 siRNA suppressed the induction of the rABCG2 mRNA level by 17β-estradiol to the same level as in untreated cells (Fig. 4a). This result suggests that this siRNA was efficiently delivered into TR-BBB13 cells and blocked the induced gene expression of rABCG2. Further study using labeled siRNA would be useful for distinguishing the transfection efficiency of siRNA from the efficacy of siRNA on endogenous rABCG2.

The rABCG2 mRNA level increased in TR-BBB13 cells following treatment with 100 nM 17β-estradiol (Fig. 4). Estrogen is thought to reach a maximum concentration of

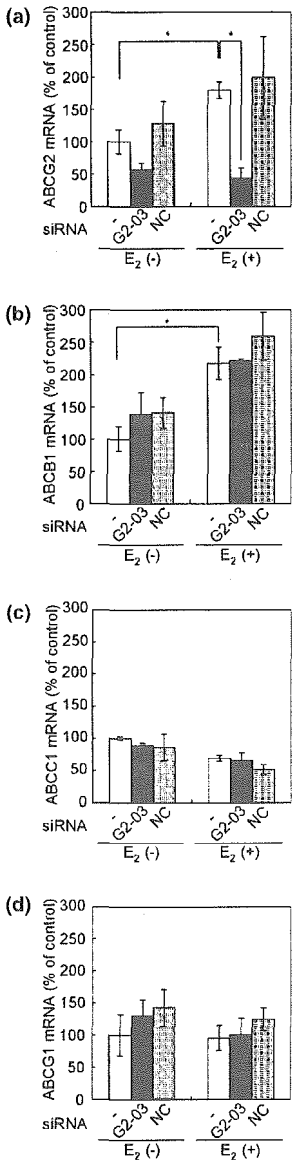

Fig. 4 Selective gene silencing of rABCG2 in TR-BBB13 cells by siRNA.TR-BBB13 cells were transfected with rABCG2 siRNA-03 (G2-03, ■) or non-specific control siRNA (NC, ▨), or untransfected (–, □). After 24 h transfection of siRNAs, the culture medium was changed to that with (+) or without (–) 17β-estradiol (E_2), and culture was continued for another 24 h. The ABCG2 (a), ABCB1 (b), ABCC1 (c), and ABCG1 (d) mRNA levels were determined by quantitative real-time PCR analysis. Each column represents the mean ± SEM ($n = 3$). Each mRNA level was normalized relative to the β-actin mRNA level. Each mRNA level is shown as percentage of the mean of the mRNA levels in TR-BBB13 cells treated with non-siRNA (–) and 17β-estradiol (E_2) (the leftmost column). $^*p < 0.05$, significant difference.

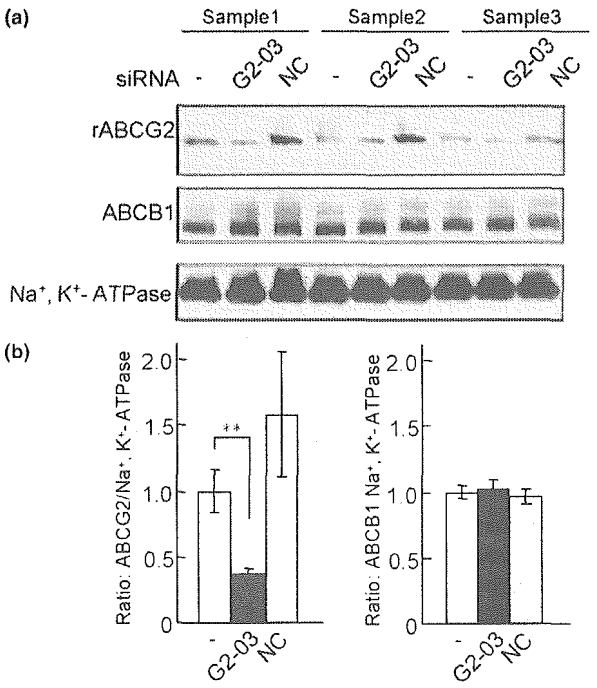

Fig. 5 Selective suppression of rABCG2 protein expression in TR-BBB13 cells by siRNA.TR-BBB13 cells were transfected with rABCG2 siRNA-03 (G2-03) or non-specific control siRNA (NC), or untransfected (–). After 36 h transfection of siRNAs, the cells were collected for western blot analysis using anti-ABCG2, anti-ABCB1 and anti-Na^+,K^+-ATPase antibodies.(a) Results from three independent western blot analyses (samples 1–3) are shown. (b) The ratio of ABCG2 (left panel) or ABCB1 (right panel) densities to Na^+,K^+-ATPase density. Each column represents the mean ± SEM ($n = 3$). $^{**}p < 0.01$, significantly different from untransfected cells (–).

150 nM during the third trimester of pregnancy (Clarke *et al.* 2001). Under such conditions, there is possibility that brain-to-blood transport activity via ABCG2 would be induced. 17β-Estradiol also regulates the expression of ABCB1 and ABCC1 mRNAs in TR-BBB13 cells, suggesting that these ABC transporter-mediated transport systems may be affected by exposure to 17β-estradiol. Recently, it has been reported that the promoter region of human ABCG2 gene contains a novel and functional estrogen response element (ERE) which has 83.3% (10 aa/12 aa) homology with a classical consensus ERE (Ee *et al.* 2004). A search of the rat genome sequence revealed that the first intron of rABCG2 also has a sequence which shows 83.3% (10 aa/12 aa) homology with the classical consensus ERE. It has been reported that 17β-estradiol enhances the ABCG2 mRNA expression in estrogen receptor (ER)-positive human cancer cell lines (Ee *et al.* 2004), and that BCECs express multiple subtypes of ER-α (Stirone *et al.* 2003). Investigation of the sensitivity of the ERE-like sequence should provide a better understanding of the mechanism of rABCG2 induction by 17β-estradiol treatment.

Introduction of siRNA into TR-BBB13 cells would be a promising approach to clarify the specific role of each transporter at the BBB because the cells retain the *in vivo*

transport properties towards various compounds (Terasaki *et al.* 2003). The efficiency of a DNA vector-based transfection using cationic liposomes was less than 5% in TR-BBB13 cells (unpublished data). The present study suggests that oligonucleotide (siRNA)-based transfection is far more effective than DNA vector-based transfection in the case of TR-BBB13 cells. ABCG2 confers multidrug resistance upon cancer cells, so ABCG2 siRNA-induced RNA interference may also be useful for overcoming drug resistance.

The luminal localization of ABCG2 at the BBB has been clearly demonstrated in humans (Cooray *et al.* 2002) and rats (Hori *et al.* 2004). However, the functional contribution of ABCG2 at the BBB *in vivo* remains unclear (Allen and Schinkel 2002). Following rABCG2 siRNA-03 transfection into TR-BBB13 cells, the mRNA level of ABCG1, which has sequence homology with ABCG2, was unchanged (Fig. 4d), and those of ABCB1 and ABCC1, which can transport some ABCG2 substrates, were unaffected for at least 48 h after the siRNA transfection (Figs 4b.c). These data suggest that the silencing effect of the siRNA is specific for the ABCG2 gene in this *in vitro* BBB model. Because the rABCG2 siRNA selectively suppressed rABCG2 mRNA and protein, the siRNA study should allow us to clarify the contribution of the transporter to the BBB efflux transport. Indeed, it has recently been reported that siRNA designed to distinguish thiamine transporter subtypes induced subtype-specific gene silencing in Caco-2 cells, and that the functional contribution of the subtypes to thiamine uptake in the cells was clearly demonstrated by using the siRNA (Said *et al.* 2004). Such a sequence-specific silencing by siRNA may be a promising way to achieve a deeper understanding of the physiological and pharmacological roles of rABCG2 at the BBB. Regarding transporter gene knockdown at the BBB, the siRNA transfection into BCECs should be more specific than suppression by inhibitors, and easier to carry out as compared with the development of knockout mice. Moreover, the siRNA technique would be useful for silencing plural transporter genes because mixtures of siRNAs can be delivered.

In conclusion, the present study has demonstrated that delivery of siRNA into this *in vitro* BBB model specifically reduced endogenous rABCG2 protein level as well as its mRNA level. Application of the siRNA technique to BBB research should increase our understanding of ABCG2 role at the BBB.

Acknowledgements

We wish to thank Prof. M. Watanabe, Mr M. Tachikawa for helpful discussion and establishment of anti-ABCG2 antibody, and Messrs M. Fujiyoshi, N. Kimura for technical assistance. We would also like to thank Ms N. Funayama for secretarial assistance. This study was supported in part by a Grant-in-Aid for Scientific Research from Japan Society for the Promotion of Science, and a 21st Century COE Program Special Research Grant from the Ministry of Education Science, Sports and Culture. It was also supported in part by the Industrial Technology Research Grant Program from the New Energy and Industrial Technology Development Organization (NEDO) of Japan.

References

Allen J. D. and Schinkel A. H. (2002) Multidrug resistance and pharmacological protection mediated by the breast cancer resistance protein (BCRP/ABCG2). *Mol. Cancer Ther.* **1**, 427–434.

Allen J. D., van Loevezijn A., Lakhai J. M., van der Valk M., van Tellingen O., Reid G., Schellens J. H., Koomen G. J. and Schinkel A. H. (2002) Potent and specific inhibition of the breast cancer resistance protein multidrug transporter in vitro and in mouse intestine by a novel analogue of fumitremorgin C. *Mol. Cancer Ther.* **1**, 417–425.

Asaba H., Hosoya K., Takanaga H., Ohtsuki S., Tamura E., Takizawa T. and Terasaki T. (2000) Blood–brain barrier is involved in the efflux transport of a neuroactive steroid, dehydroepiandrosterone sulfate, via organic anion transporting polypeptide 2. *J. Neurochem.* **75**, 1907–1916.

de Bruin M., Miyake K., Litman T., Robey R. and Bates S. E. (1999) Reversal of resistance by GF120918 in cell lines expressing the ABC half-transporter, MXR. *Cancer Lett.* **146**, 117–126.

Clarke R., Leonessa F., Welch J. N. and Skaar T. C. (2001) Cellular and molecular pharmacology of antiestrogen action and resistance. *Pharmacol. Rev.* **53**, 25–71.

Cooray H. C., Blackmore C. G., Maskell L. and Barrand M. A. (2002) Localisation of breast cancer resistance protein in microvessel endothelium of human brain. *Neuroreport* **13**, 2059–2063.

Ee P. L., Kamalakaran S., Tonetti D., He X., Ross D. D. and Beck W. T. (2004) Identification of a novel estrogen response element in the breast cancer resistance protein (ABCG2) gene. *Cancer Res.* **64**, 1247–1251.

Elbashir S. M., Harborth J., Weber K. and Tuschl T. (2002) Analysis of gene function in somatic mammalian cells using small interfering RNAs. *Methods* **26**, 199–213.

Gao B., Stieger B., Noe B., Fritschy J. M. and Meier P. J. (1999) Localization of the organic anion transporting polypeptide 2 (Oatp2) in capillary endothelium and choroid plexus epithelium of rat brain. *J. Histochem. Cytochem.* **47**, 1255–1264.

Hannon G. J. (2002) RNA interference. *Nature* **418**, 244–251.

Hori S., Ohtsuki S., Tachikawa M., Kimura N., Kondo T., Watanabe M., Nakashima E. and Terasaki T. (2004) Functional expression of rat ABCG2 on the luminal side of brain capillaries and its enhancement by astrocyte-derived soluble factor(s). *J. Neurochem.* **90**, 526–536.

Hosoya K., Takashima T., Tetsuka K. *et al.* (2000a) mRNA expression and transport characterization of conditionally immortalized rat brain capillary endothelial cell lines; a new *in vitro* BBB model for drug targeting. *J. Drug Target.* **8**, 357–370.

Hosoya K., Tetsuka K., Nagase K. *et al.* (2000b) Conditionally immortalized brain capillary endothelial cell lines established from a transgenic mouse harboring temperature-sensitive simian virus 40 large T-antigen gene. *AAPS Pharmsci.* **2**, article 27, doi: 10.128/ps020327 Available: http://www.aapspharmsci.org

Hosoya K., Ohtsuki S. and Terasaki T. (2002) Recent advances in the brain-to-blood efflux transport across the blood–brain barrier. *Int. J. Pharm.* **248**, 15–29.

Hyafil F., Vergely C., Du Vignaud P. and Grand-Perret T. (1993) *In vitro* and *in vivo* reversal of multidrug resistance by GF120918, an acridonecarboxamide derivative. *Cancer Res.* **53**, 4595–4602.

Mori S., Takanaga H., Ohtsuki S., Deguchi T., Kang Y. S., Hosoya K. and Terasaki T. (2003) Rat organic anion transporter 3 (rOAT3) is responsible for brain-to-blood efflux of homovanillic acid at the abluminal membrane of brain capillary endothelial cells. *J. Cereb. Blood Flow Metab.* **23**, 432–440.

Nabokina S. M., Ma T. Y. and Said H. M. (2004) Mechanism and regulation of folate uptake by the human pancreatic epithelial MIA PaCa-2 cells. *Am. J. Physiol. Cell Physiol.* **287**, C142–C148.

Rabindran S. K., Ross D. D., Doyle L. A., Yang W. and Greenberger L. M. (2000) Fumitremorgin C reverses multidrug resistance in cells transfected with the breast cancer resistance protein. *Cancer Res.* **60**, 47–50.

Reynolds A., Leake D., Boese Q., Scaringe S., Marshall W. S. and Khvorova A. (2004) Rational siRNA design for RNA interference. *Nat. Biotechnol.* **22**, 326–330.

Said H. M., Balamurugan K., Subramanian V. S. and Marchant J. S. (2004) Expression and functional contribution of hTHTR-2 in thiamine absorption in human intestine. *Am. J. Physiol. Gastrointest. Liver Physiol.* **286**, G491–G498.

Stirone C., Duckles S. P. and Krause D. N. (2003) Multiple forms of estrogen receptor-alpha in cerebral blood vessels: regulation by estrogen. *Am. J. Physiol. Endocrinol. Metab.* **284**, E184–E192.

Suzuki M., Suzuki H., Sugimoto Y. and Sugiyama Y. (2003) ABCG2 transports sulfated conjugates of steroids and xenobiotics. *J. Biol. Chem.* **278**, 22 644–22 649.

Terasaki T. and Hosoya K. (1999) The blood–brain barrier efflux transporters as a detoxifying system for the brain. *Adv. Drug Deliv. Rev.* **36**, 195–209.

Terasaki T., Ohtsuki S., Hori S., Takanaga H., Nakashima E. and Hosoya K. (2003) New approaches to *in vitro* models of blood–brain barrier drug transport. *Drug Discov. Today* **8**, 944–954.

Virgintino D., Robertson D., Errede M., Benagiano V., Girolamo F., Maiorano E., Roncali L. and Bertossi M. (2002) Expression of P-glycoprotein in human cerebral cortex microvessels. *J. Histochem. Cytochem.* **50**, 1671–1676.

Wu H., Hait W. N. and Yang J. M. (2003) Small interfering RNA-induced suppression of MDR1 (P-glycoprotein) restores sensitivity to multidrug-resistant cancer cells. *Cancer Res.* **63**, 1515–1519.

Yoshinari K., Miyagishi M. and Taira K. (2004) Effects on RNAi of the tight structure, sequence and position of the targeted region. *Nucl Acids Res.* **32**, 691–699.

Zelcer N., Reid G., Wielinga P., Kuil A., van der Heijden I., Schuetz J. D. and Borst P. (2003) Steroid and bile acid conjugates are substrates of human multidrug-resistance protein (MRP)4 (ATP-binding cassette C4). *Biochem. J.* **371**, 361–367.

Zhang Y., Boado R. J. and Pardridge W. M. (2003) *In vivo* knockdown of gene expression in brain cancer with intravenous RNAi in adult rats. *J. Gene Med.* **5**, 1039–1045.

Nitric Oxide Inhibits IFN-α Production of Human Plasmacytoid Dendritic Cells Partly via a Guanosine 3′,5′-Cyclic Monophosphate-Dependent Pathway[1]

Rimpei Morita,[2]*† Takashi Uchiyama,* and Toshiyuki Hori[3]*

NO, a free radical gas, is known to be critically involved not only in vascular relaxation but also in host defense. Besides direct bactericidal effects, NO has been shown to inhibit Th1 responses and modulate immune responses in vivo, although the precise mechanism is unclear. In this study, we examined the effect of NO on human plasmacytoid dendritic cells (pDCs) to explore the possibility that NO might affect innate as well as adaptive immunity through pDCs. We found that NO suppressed IFN-α production of pDCs partly via a cGMP-dependent mechanism, which was accompanied by down-regulation of IFN regulatory factor 7 expression. Furthermore, treatment of pDCs with NO decreased production of IL-6 and TNF-α and up-regulated OX40 ligand expression. In accordance with these changes, pDCs treated with NO plus CpG-oligodeoxynucleotide AAC-30 promoted differentiation of naive CD4$^+$ T cells into a Th2 phenotype. Moreover, pDCs did not express inducible NO synthase even after treatment with AAC-30, LPS, and several cytokines. These results suggest that exogenous NO and its second messenger, cGMP, alter innate as well as adaptive immune response through modulating the functions of pDCs and may be involved in the pathogenesis of certain Th2-dominant allergic diseases. *The Journal of Immunology,* **2005, 175: 806–812.**

Nitric oxide, a free-radical gas, is an important regulator and mediator of a wide range of physiological processes, including blood vessel relaxation, apoptosis, inflammation, and macrophage-mediated cytotoxicity for microbes and tumor cells (1–3). Most of the biological effects of NO are thought to be mediated by the cytoplasmic soluble guanylyl cyclase (GC)[4] that catalyzes biosynthesis of intracellular cGMP (1, 4). Evidence has indicated that NO not only exhibits protective activity against various infections but also regulates adaptive immunity by affecting the balance of Th1/Th2 responses. The inducible NO synthase (iNOS)-deficient or -mutant mice have been reported to mount significantly stronger Th1 responses than the wild-type mice with reduced virus titers, as well as pathological consequences of influenza A virus-induced pneumonia (5), whereas these mice are highly susceptible to several intracellular pathogens, including *Leishmania major*, *Mycobacterium tuberculosis*, and *Listeria monocytogenes* (6–8). Treatment with selective iNOS or NOS inhibitors has been shown to alleviate the pathological consequences not only of various virus infections, such as HSV-1-induced pneumonia and coxsackievirus B3-induced myocarditis (9, 10) but also of allergic diseases. For example, NOS inhibitors reduce the number of eosinophils infiltrated in lung tissues in sensitized rodents (2, 11, 12). Moreover, it is known that treatment with NO donors decreases IFN-γ production in mice. These findings suggest that NO affects adaptive immunity with an apparent inclination toward inhibition of Th1 responses.

Dendritic cells (DCs) are the most potent APCs playing a pivotal role in the induction of primary immune responses (13, 14). Certain pathogen-derived compounds, cytokines, and soluble mediators have been shown to induce differentiation of immature DCs into mature DCs of a polarized phenotype toward Th1 or Th2 responses (13, 14). In humans, two distinct subsets of primary DCs are identified in peripheral blood and tonsils according to the difference in expression of CD11c (15, 16). While CD11c$^-$ myeloid DCs produce IL-12 through TLR-2 and -4 signaling, CD11c$^-$ plasmacytoid DCs (pDCs) secrete high levels of type I IFNs (IFN-$\alpha\beta$) in response to viral infection presumably involving TLR-7 and -9 (17–19). Type I IFNs play essential roles in antiviral innate immunity by inhibiting viral replication in infected cells and by augmenting DC as well as NK cell function (20, 21). Thus, pDCs are crucial effecter cells, which are the major source of type I IFNs and can modulate both innate and adaptive immunity (22).

The role of NO in adaptive immunity in humans is less clear. Nevertheless, recent clinical studies have indicated that exhaled NO is increased in certain allergic diseases such as bronchial asthma, nasal allergy, and atopic dermatitis, suggesting that NO may be involved in Th2 predominance in these disorders (23–26). Thus, it is important to dissect the cellular and molecular mechanisms by which NO affects the direction of immune response. In the present study, we focused on human pDCs and investigated whether NO altered their cytokine production and the consequent Th1/Th2 cell polarization upon stimulation with a TLR-9 ligand because pDCs have been reported to accumulate in nasal mucosa after allergic challenge in humans (27). Herewith, we show that NO suppresses the production of IFN-α of pDCs and polarizes them toward a Th2-promoting phenotype partly via a cGMP-dependent pathway.

*Department of Hematology and Oncology and †Horizontal Medical Research Organization, Graduate School of Medicine, Kyoto University, Kyoto, Japan

Received for publication December 28, 2004. Accepted for publication May 16, 2005.

The costs of publication of this article were defrayed in part by the payment of page charges. This article must therefore be hereby marked *advertisement* in accordance with 18 U.S.C. Section 1734 solely to indicate this fact.

[1] This work was supported in part by grants-in-aid from the Ministry of Education, Culture, Sports, Science, and Technology of Japan.

[2] Current address: Baylor Institute for Immunology Research, Dallas, TX 75204.

[3] Address correspondence and reprint requests to Dr. Toshiyuki Hori, Department of Hematology and Oncology, Graduate School of Medicine, 54 Shogoin Kawara-cho, Sakyo-ku, Kyoto 606-8507, Japan. E-mail address: thori@huhp.kyoto-u.ac.jp

[4] Abbreviations used in this paper: GC, guanylyl cyclase; iNOS, inducible NO synthase; NOS, NO synthase; DC, dendritic cell; pDC, plasmacytoid DC; DETA/NO, 2,2′-(hydroxynitrosohydrazono)bis-ethanimine; ODQ, *H*-(1,2,4)oxadiazolo(4,3-α)quinoxalin-1-one; db-cGMP, dibutyryl-cGMP; IRF-7, IFN regulatory factor-7; OX40L, OX40 ligand; MFI, mean fluorescence intensity.

0022-1767/05/$02.00

Materials and Methods

Media and reagents

RPMI 1640 supplemented with 10% heat-inactivated FBS (Invitrogen Life Technologies) was used throughout the experiments. 2,2'-(Hydroxynitrosohydrazono)bis-ethanimine (DETA/NO) (0.5 to 50 μM), *H*-(1,2,4)oxadiazolo(4,3-α)quinoxalin-1-one (ODQ) (3 μM), 8-pCPT-cGMP (10^{-5} to 10^{-3} M), and LPS (*Salmonella typhimurium*) (1 μg/ml) were purchased from Sigma-Aldrich. Dibutylyl-cGMP (db-cGMP) (10^{-5} to 10^{-3} M) was purchased from Nacalai Tesque. TGF-β (10 ng/ml), IFN-γ (100 U/ml), and TNF-α (0.8 μg/ml) were purchased from PeproTech. CpG-oligodeoxynucleotide AAC-30 (5 μM) was synthesized by Biologica (17).

Purification of human pDCs and their culture

Peripheral blood buffy coats were obtained from healthy human donors (kindly provided by the Kyoto Prefectural Red Cross Blood Center). PBMCs were isolated by Ficoll-Paque (Amersham Biosciences) density gradient centrifugation. pDCs were isolated from PBMCs with MACS magnetic bead columns using the BDCA-4 Cell Isolation kit (Miltenyi Biotec). The purity of pDCs was estimated as that of $CD123^+$ cells and accounted for >96% of the isolated cells. pDCs were cultured at 5×10^5 cells/ml up to for 36 h.

Western blot analysis of IFN regulatory factor (IRF)-7

pDCs were incubated in the culture medium with or without AAC-30, DETA/NO, ODQ, or db-cGMP (10^{-3} M) in 24-well plates at 5×10^5 cells in 1 ml of medium/well. After 6 h, pDCs were collected, washed twice with PBS, and lysed in 60 μl of SDS sample buffer/sample. The cell lysates were subjected to SDS-PAGE with 10% polyacrylamide gel. Then the samples were transferred to Immobilon-P polyvinylidene difluoride membranes (Millipore) and incubated sequentially with polyclonal anti-IRF-7 or polyclonal anti-β-actin Abs (Santa Cruz Biotechnology) and with HRP-conjugated second Abs (Amersham Biosciences). IRF-7 and β-actin proteins were visualized using ECL detection kit (Amersham Biosciences). Relative signal intensities of IRF-7 compared with that of β-actin were quantified by densitometry, in which the value of freshly isolated pDCs was set as 100%.

Flow cytometric analysis of cell surface Ags

pDCs were stimulated with AAC-30 in the presence or absence of DETA/NO. After 21 h, cells were collected and stained with the following FITC-conjugated mAbs: anti-HLA-DR (BD Biosciences), anti-CD80, and anti-CD86 (Immunotech). For the detection of OX40 ligand (OX40L), stimulated cells were incubated with biotinylated anti-OX40L mAb, ik-1 (28), for 30 min followed by PE-conjugated streptavidin. After immunofluorescence staining, cells were analyzed with a FACScan flow cytometer (BD Biosciences) using CellQuest software (BD Biosciences). The expression level of each Ag was indicated as Δ mean fluorescence intensity (ΔMFI), which was calculated by subtraction of MFI of the control value from that of the specific mAb.

Apoptosis detection

After 36 h of culture in the absence or presence of the indicated stimuli in 48-well plates at 2.5×10^5 cells in 500 μl of medium/well, the cells were stained with propidium iodide (Molecular Probes) and FITC-conjugated annexin V (Caltag Laboratories) and analyzed with a FACScan flow cytometer (BD Biosciences) using CellQuest software (BD Biosciences).

Analysis of intracellular cytokine production

Naive $CD4^+$ T cells were purified from umbilical cord blood mononuclear cells of healthy neonates by MACS using a MACS $CD4^+$ T Cell Isolation Kit II (Miltenyi Biotec). $CD45RA^+CD4^+$ cells accounted for >95% of the isolated cells. pDCs (1×10^5 cells/well) that had been pretreated with the indicated reagents were washed thoroughly, irradiated (30 Gy), and cocultured with allogeneic naive $CD4^+$ T cells (1×10^6 cells/well) in 24-well plates for 7 days. Then cells were collected and stimulated with 50 ng/ml PMA (Sigma-Aldrich) and 500 ng/ml ionomycin (Calbiochem) for 5 h. Brefeldin A (10 μg/ml) (Sigma-Aldrich) was added for the last 2 h. Cells were fixed with 2% formalin, permeabilized with PBS containing 2% FBS and 0.5% saponin, and then stained with FITC-anti-IFN-γ mAb and PE-anti-IL-4 mAb (BD Biosciences). Stained cells were analyzed with a FACScan (BD Biosciences).

Measurement of cytokines by ELISA

pDCs were cultured with AAC-30 in the absence or presence of DETA/NO, ODQ, or cGMP analogues in 96-well, round-bottom plates at 1×10^5 cells in 200 μl of medium/well. After 21 h, each supernatant was harvested, and cytokine concentrations in the supernatants were measured by the sandwich ELISA using matched paired Abs specific for IL-6, IL-10, IFN-α, and TNF-α (BioSource International), according to the manufacturer's instructions.

Detection of iNOS expression and NO production

pDCs and human monocyte cell line THP-1 were incubated in the medium with the indicated stimuli in 48-well plates at 2.5 and 1.25×10^5 cells in 500 μl of medium/well, respectively. After 18 h, cells and the supernatants were collected. For detection of iNOS expression, cells were lysed in 80 μl of SDS sample buffer/sample and subjected to SDS-PAGE with 10% polyacrylamide gel. Then the samples were transferred to Immobilon-P polyvinylidene difluoride membranes (Millipore) and incubated sequentially with monoclonal anti-iNOS or polyclonal anti-β-actin Abs (Santa Cruz Biotechnology) and with HRP-conjugated second Abs (Amersham Biosciences).

NO was measured as nitrite using the Griess reaction. Briefly, 100 μl of modified Griess reagent (Sigma-Aldrich) were added to 100 μl of the supernatants. After 15 min, absorbance was measured at 540 nm. The nitrite content in the samples was calculated based on a standard curve read from a prepared standard solutions of sodium nitrite.

Statistical analysis

Statistical analyses were performed by Student's *t* test, one-way ANOVA, or paired *t* test. Values of $p < 0.05$ were considered to be statistically significant.

Results

NO suppresses IFN-α production of pDCs partly via cGMP-dependent mechanism

Because several reports indicated that NO was involved in the inhibition of Th1 responses (2, 3, 5, 6), first, we examined whether NO would have any influence on IFN-α production of pDCs. We cultured pDCs with the TLR-9 ligand, AAC-30, in the absence or presence of the NO donor, DETA/NO, for 21 h and measured IFN-α concentrations in the supernatants with ELISA. As shown Fig. 1*A*, AAC-30-stimulated pDCs produced large amounts of IFN-α, which was suppressed by treatment with DETA/NO in a dose-dependent manner up to 90% suppression at 50 μM DETA/NO. The addition of a specific soluble GC inhibitor, ODQ, partly restored these cytokine productions of AAC-30 plus DETA/NO-treated pDCs (Fig. 1*B*). Two kinds of membrane-permeable cGMP analogues, 8-pCPT-cGMP and db-cGMP, reduced the production of IFN-α of pDCs in a dose-dependent manner (Fig. 1*C*). These results indicated that NO suppressed IFN-α production of pDCs, and this effect was in part mediated by cGMP-dependent mechanism.

NO suppresses IRF-7 expression of pDCs via a cGMP-dependent mechanism

Next, we analyzed the mechanism by which NO suppresses IFN-α production of pDCs. We focused on the level of IRF-7 expression that is the critical determinant of the transcriptional activation of the *IFN-α* gene (29, 30 and examined the effect of NO on the expression of IRF-7 in AAC-30-treated pDCs by Western blot analysis. As previously reported, freshly isolated pDCs constitutively expressed IRF-7 to some extent, and treatment with AAC-30 for 6 h increased the expression levels of IRF-7 in pDCs (31, 32). As shown in Fig. 2, the addition of DETA/NO to AAC-30-treated pDCs decreased the expression levels of IRF-7 to the almost same levels as that of fresh pDCs, and ODQ restored the expression levels of IRF-7 in AAC-30 plus DETA/NO-treated pDCs. The addition of db-cGMP (10^{-3} M) to AAC-30-treated pDCs also decreased the expression levels of IRF-7. Because these changes coincided with the changes in IFN-α production of pDCs (Fig. 1, *A–C*), the suppression of IFN-α production by NO seems to be

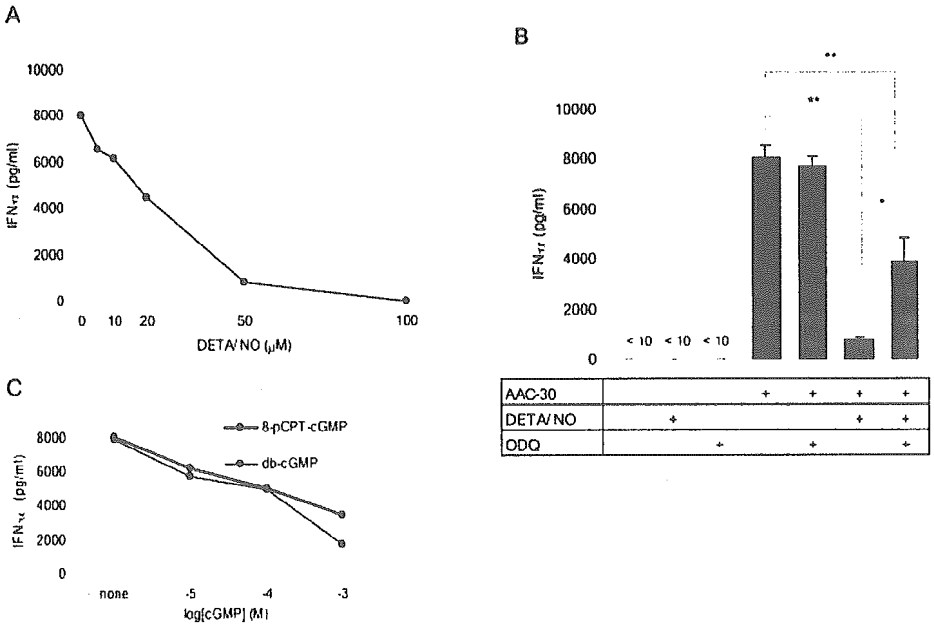

FIGURE 1. Effects of NO and cGMP on production of IFN-α of AAC-30-stimulated pDCs. *A*, pDCs were stimulated with AAC-30 (5 μM) in the absence or presence of DETA/NO (5–100 μM) for 21 h. The concentrations of IFN-α of pDC culture supernatants were measured by ELISA. *B*, pDCs were stimulated with or without AAC-30 (5 μM) in the absence or presence of DETA/NO (50 μM) or ODQ (3 μM) for 21 h. The concentrations of IFN-α of pDC culture supernatants were measured by ELISA. The results are shown as the mean ± SD of three independent experiments. **, $p < 0.01$; and *, $p < 0.05$; Student's *t* test. *C*, pDCs were stimulated with AAC-30 (5 μM) in the absence or presence of membrane-permeable cGMP analogues, 8-pCPT-cGMP or db-cGMP (10^{-5} to 10^{-3} M), for 21 h. The concentrations of IFN-α were measured by ELISA. The results shown are from one representative experiment of three consistent ones.

mostly mediated by down-regulation of IRF-7 expression via a cGMP-dependent pathway.

NO suppresses other inflammatory cytokine production of pDCs

To investigate whether NO affects the production of inflammatory as well as anti-inflammatory cytokines of pDCs, we cultured pDCs under the same conditions as Fig. 1*A* for 21 h and measured the concentrations of IL-6, TNF-α, and IL-10 in the culture supernatants by ELISA. Although unstimulated pDCs did not produce any of these cytokines, AAC-30 stimulation induced production of IL-6 and TNF-α but not IL-10 of pDCs as reported previously (16–18). The treatment with DETA/NO significantly reduced the production of IL-6 and TNF-α of AAC-30-stimulated pDCs, and the addition of ODQ partly restored the production of these cytokines (Fig. 3).

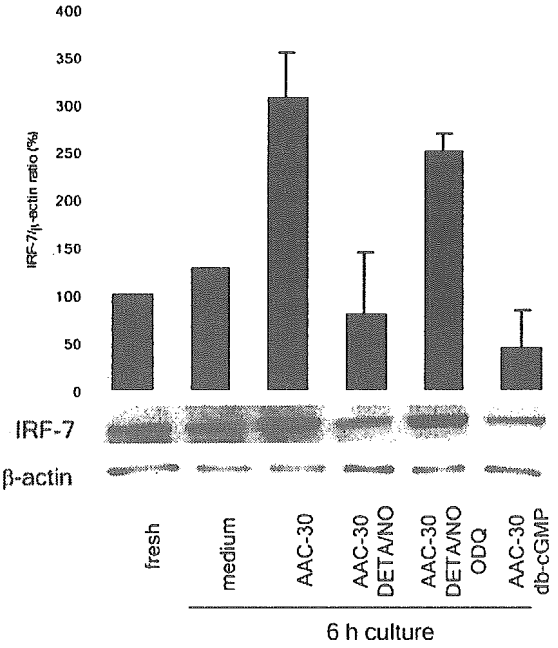

FIGURE 2. Effects of NO and cGMP on IRF-7 expression in AAC-30-stimulated pDCs. pDCs were stimulated with or without AAC-30 (5 μM) in the absence or presence of DETA/NO (50 μM), ODQ (3 μM), or db-cGMP (10^{-3} M) for 6 h. Expression of IRF-7 and β-actin, an internal protein control, was evaluated by Western blot analysis. The data of one representative experiment of three consistent ones are shown in the *lower panel*. The *upper bar graph* indicates relative signal intensities of IRF-7. The value of freshly isolated pDCs is set as 100%. The results are shown as the mean ± SD of the three experiments.

NO up-regulates the expression level of OX40L on pDCs in the presence of AAC-30

Next, we examined the effects of NO on the phenotypic maturation of pDCs with AAC-30. pDCs were cultured with AAC-30 in the absence or presence of DETA/NO for 21 h and then subjected to the flow cytometric analysis. The addition of DETA/NO to AAC-30 hardly changed the expression levels of CD80, CD86, or HLA-DR on pDCs (Fig. 4*A*). In contrast, stimulation with DETA/NO in the presence of AAC-30 resulted in significant up-regulation of OX40L (Fig. 4*B*), which has been reported to critically contribute to Th2 responses (33, 34).

NO has little effect on apoptosis of pDCs in the presence of AAC-30

NO is known to have proapoptotic or antiapoptotic properties, depending on cell types (2, 35). Although it has been reported recently that NO has antiapoptotic effects on myeloid DCs stimulated with LPS (36), it is not yet clear whether NO has any effect on apoptosis of pDCs. To address this question, we incubated pDCs with or without AAC-30 in the absence or presence of a variety concentrations of DETA/NO (0.5–50 μM) for 36 h and measured percentages of dead cells, as well as early apoptotic cells by flow cytometry. As shown Fig. 5, *A* and *B*, while the treatment with AAC-30 alone significantly reduced the percentages of dead cells of pDCs, the addition of DETA/NO hardly affected those of dead and early apoptotic cells of pDCs, indicating that NO had little proapoptotic effects on pDCs at least in the presence of AAC-30. Thus, it is likely that the decreases in cytokine productions of pDCs were caused by the decrease in the individual cellular ability to secrete cytokines rather than that in the numbers of cytokine-producing pDCs.

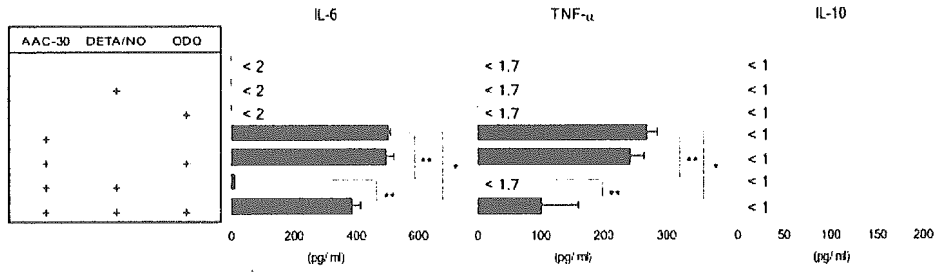

FIGURE 3. Effects of NO on production of IL-6, TNF-α, and IL-10 of AAC-30-stimulated pDCs. pDCs were stimulated with or without AAC-30 (5 μM) in the absence or presence of DETA/NO (50 μM) or ODQ (3 μM) for 21 h. The concentrations of IL-6, TNF-α, and IL-10 of pDC culture supernatants were measured by ELISA. The results are shown as the mean ± SD of three experiments. **, $p < 0.01$; *, $p < 0.05$; Student's t test.

NO polarizes pDCs toward a Th2-promoting phenotype

Because NO suppressed IFN-α production of pDCs and up-regulated OX40L expression on pDCs (Figs. 1*A* and 4*B*), we next investigated whether NO could polarize pDCs toward a Th1- or Th2-promoting phenotype. To address this question, we cocultured allogeneic naive $CD4^+$ T cells with pDCs stimulated with AAC-30 in the absence or presence of DETA/NO (50 μM). Then, $CD4^+$ T cells were analyzed for intracellular production of IFN-γ as well as IL-4 by flow cytometry. Although coculture with AAC-30-activated pDCs generated large amounts of IFN-γ-producing T cells, the treatment of AAC-30-stimulated pDCs with DETA/NO resulted in less IFN-γ-producing T cells and more IL-4-producing T cells (*Fig. 6, A* and *B*). These results indicated that NO polarized pDCs toward a Th2-promoting phenotype.

Treatment with TLR ligands and cytokines induces pDCs neither to express iNOS nor to produce NO

According to several reports, human myeloid DCs neither express iNOS nor produce NO in the presence of inflammatory cytokines

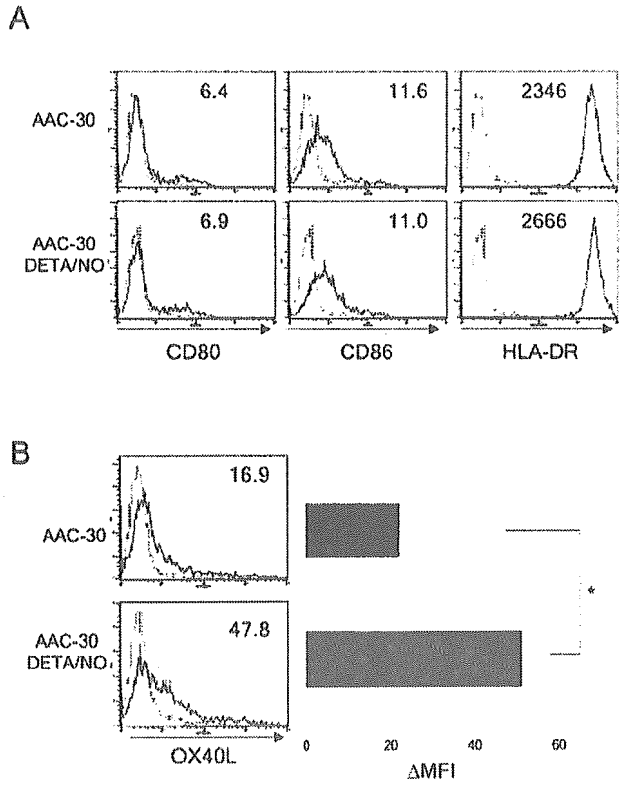

FIGURE 4. Effects of NO on phenotypic changes of AAC-30-stimulated pDCs. pDCs were stimulated with AAC-30 (5 μM) in the absence or presence of DETA/NO (50 μM) for 21 h, and the changes of expression of CD80, CD86, HLA-DR (*A*), and OX40L (*B, left*) were analyzed with a FACScan. The staining profiles with specific mAbs and isotype-matched controls are shown in solid and dotted line histograms, respectively. The number in each histogram profile indicates ΔMFI. The results shown are from one representative experiment of three consistent ones. *B* (*right*). The expression level of OX40L on pDCs is indicated as the mean ± SD of the three experiments. *, $p < 0.05$; Student's t test.

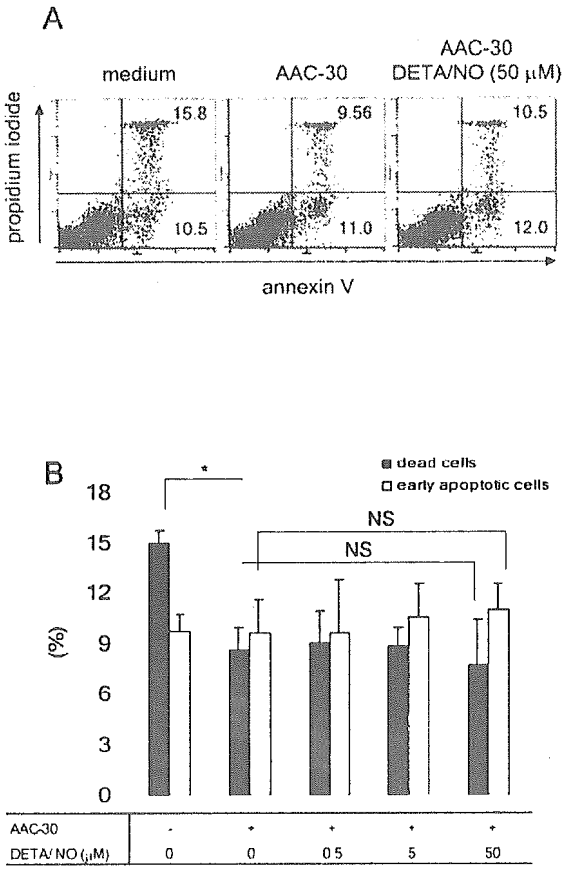

FIGURE 5. Effects of NO on apoptosis of pDCs. pDCs were cultured with or without AAC-30 (5 μM) in the absence or presence of DETA/NO (0.5–50 μM) for 36 h. Then cells were collected, stained with propidium iodide and annexin V, and analyzed with a FACScan. *A*, Dot plots of a representative experiment are shown. Numbers in the *upper* and *lower right quadrants* indicate percentages of dead and early apoptotic cells, respectively. *B*, Data are shown as the mean ± SD of four independent experiments. **, $p < 0.05$; one-way ANOVA.